Fall 2007

Bridge damage detection using an intelligent engineering system

Dionysios N. Danilatos

Department:

BRIDGE DAMAGE DETECTION

USING

AN INTELLIGENT ENGINEERING SYSTEM

by

DIONYSIOS N. DANILATOS

A THESIS

Presented to the Faculty of the Graduate School of the

UNIVERSITY OF MISSOURI-ROLLA

In Partial Fulfillment of the Requirements for the Degree

MASTER OF SCIENCE IN ENGINEERING MANAGEMENT

2007

Approved by

_____	_____
Cihan H. Dagli, Advisor	David Enke

_____

Ashraf Ayoub

ABSTRACT

This thesis attempts to improve the practical and effective incorporation of Smart Engineering Architectures into Health Monitoring Systems for civil bridges. The designed Damage Diagnostic Algorithm is inspired by a reductionistic model from the Cognitive Psychology that describes the Human Mental Processes.

Prior research efforts attempted to apply Artificial Neural Networks, especially Backpropagation, in order to perform Structural Damage Diagnosis. However, the Neuro-Computing methods have a number of inefficiencies, as the lack of generalization, and the difficulties to collect the optimum datasets. In this thesis, to overcome these problems, two innovative software components aim to improve the training and testing datasets for the learning algorithm. The obtained datasets exhibit properties (e.g. diversity and network performance quality) that have statistical significance. The two proposed procedures are not necessarily applied to the Damage Diagnostics Systems only, but they might be extended as a universal improvement for Backpropagation or for Networks that employ supervised learning, in general.

The designed Damage Diagnostic System is tested on simulated data. It is demonstrated that the method is very sensitive in detecting mild linear damage. Two important advantages of the Diagnostic System are the prediction accuracy and the flexibility.

ACKNOWLEDGMENTS

I am grateful to one of the most remarkable persons I ever met, my advisor Dr. Cihan H. Dagli, who happens to be an outstanding personality in the area of Artificial Neural Networks and a charismatic mentor at the same time. Although we trace our descents from two historically adversary countries[1], the rivalry of whom perpetuates a legacy of suspicion among their citizen, Dr. Dagli stands out from this. Dr. David Enke who also serves in this committee is equally thanked for the knowledge he shared with me through coursework and discussions. Many thanks to Dr. Ashraf Ayoub who came from the Civil Engineering Department as a deus ex machina to contribute his expertise and suggestions. Also, acknowledgments go to Dr. Antonio Nanni for attracting research funds from the Federal Railway Agency, but especially for his wonderful lectures that inspired me to continue my graduate studies in Civil Engineering.

I feel an obligation to the Greek State Scholarship Foundation (I.K.Y) that sponsored my studies. I wish to express my deep appreciation to my academic supervisor Dr. Errikos Mouratidis for his enlightening advice and especially for his encouragement during the stressful first period of my studies abroad. I want also to thank Ms. Adamantiadou, Ms. Metaxa and Mr. Mastrokallos, administrative employees of the aforementioned foundation, for their continuous support.

Huge thanks to the following researchers for the smooth collaboration during the Mac Arthur Railway Bridge Project: Dr. Pedro Silva, Dr. Hardy Pottinger, Mr. Thomas Burns, Dr. Hailin Li, Mr. José Mata, Dr. Lakshmanan Meyyappan, Mrs. Anja Frauenberger, and Mr. Xiangdong Liu. I feel very fortunate that the UMR employees Mses. Krista Chambers and Vicki Hudgins went the extra mile, in order to handle my case. I feel a sense of gratitude to Dr. Nil Hande Ergin and Mr. Renzhong Wang for their help in the thesis submission. I am also deeply grateful to my parents, Nikos and Hara, who, throughout my childhood, instilled in me the faith that seeking education is not just a means of gaining more money, but the quintessence of a human being.

---

[1] Certain scholars insist to classify the dipole of Greece and Turkey as a paradigm of the so-called "Clash of Civilizations"! (Stearns M. 2000 and Huntington S. 1996).

TABLE OF CONTENTS

LIST OF ILLUSTRATIONS

LIST OF TABLES

NOMENCLATURE

Some symbols denote different variables; however they are distinguished when the subscripts are applied.

Symbol	Description
$\mathbf{z}_{trn}$	Mid-span displacement training array
$\ddot{\mathbf{z}}_{trn}$	Beam Acceleration Training array
$\mathbf{p}_{trn}$	Excitation load array, as measured and used for training the A-Class Neuro-Fuzzy Network
$e_{pred,trn}$	Average prediction error of the A-Class Neuro-Fuzzy Networks in the prediction of the training dataset
$\delta_{pred,trn}$	Average predicted damage rate
$\mathbf{p}_{pred,trn}$	Predicted bridge excitation
$\mathbf{p}_{o}$	Vibration amplitude array
$\boldsymbol{\omega}_{\mathbf{o}}$	Vibration frequency array
$\delta'_{pred,j}$	Corrected predicted damage rate, which is calculated with sampled measurements from the vehicle event *j*
j	Index that denotes the vehicle event
K_j	Stiffness Matrix
$e_{pred,j}$	Average prediction error of F different A-Class Neuro-Fuzzy Networks, for vehicle event j. This average error is estimated by the B-Class Neuro-Fuzzy Network.
F	The amount of the pages in the A-Class ANFIS datasets, which equals the number of the sampling measurements during each passage of the moving load along the beam
R	The amount of the rows in the datasets for A-Class ANFIS
N_{trn}	Size of the training dataset
$N_{max,trn}$	Ceiling limit for the training dataset
$N_{min,trn}$	Bottom limit for the training dataset
z_{min}	The minimum value that an element in deflection array might take potentially, during the service life of the bridge

z_{max}	The maximum value that an element in deflection array might take potentially, during the service life of the bridge
$\ddot{z}_{min}$	The minimum value that an element in the acceleration array might take potentially, during the service life of the bridge
$\ddot{z}_{max}$	The maximum value that an element in the acceleration array might take potentially, during the service life of the bridge
z	Element of the array **z**
$\ddot{z}$	Element of the array $\ddot{\mathbf{z}}$
p	Element of the array **p**
$\ddot{z}$	Element of the array $\ddot{\mathbf{z}}$
p(t)	Discrete value of the excitation force, at the time moment t
p_{max}	The most severe vehicle loading that the bridge might carry potentially, during its service life
$\{p_{max,1}, p_{max,2} \ldots, p_{max,n}\}$	The most severe combination of the spatial vehicle loadings that bridge might carry potentially, during its service life
$p_{o,max}$	Maximum load amplitude
$\omega_{o,max}$	Maximum load frequency
p_{min}	Minimum excitation load
$[p_{o,min}, p_{o,max}]$	Interval range between the probable minimum and maximum load amplitude values
$[\omega_{o,min}, \omega_{o,max}]$	Interval range between the probable minimum and maximum load frequency values
P_r	The probability function
Ω_z	The sample space that includes all the potential values of z
$\Omega_{\ddot{z}}$	The sample space that includes all the potential values of $\ddot{z}$
$\overline{e}_{trn}$	Root-mean square of errors e_j, calculated for the training dataset
σ_{trn}	Variance of errors e_j, calculated for the training dataset
$\overline{e}_{chk}$	Root-mean square of errors e_j, calculated for the checking dataset

σ_{chk}	Variance of errors e_j, calculated for the checking dataset
$\bar{e}_{\lim,trn}$	Imposed limit on the root-mean-square of errors e_j, calculated for the training dataset
$\bar{e}_{\lim,chk}$	Imposed limit on the root-mean-square of errors e_j, calculated for the checking dataset
$\bar{e}_{\lim}$	Imposed limit on the root-mean-square of errors e_j
$\sigma_{\lim}$	Imposed limit on the variance of errors e_j
$\mathbf{S}(s_p)$	Array that contains the rows of the training dataset, sorted from the smallest to the biggest, with respect to selected array $\mathbf{z}$ or $\ddot{\mathbf{z}}$
$A=[\mathbf{z_r},\ \ddot{\mathbf{z}}\ \mathbf{p_o},\ \boldsymbol{\omega_o}]$	Training dataset
s_p	A binary parameter that takes the value of 1 for selected array $\mathbf{z}$ or the value 2 for selected array $\ddot{\mathbf{z}}$
$\mathbf{S_Q}$	Array of sorted deflection data
$\mathbf{S_{aux,\,Q}}$	Auxiliary array
$\mathbf{D}$	Array in which the hth element represents the distance of h^{th} element $S_{h,}$of array $\mathbf{S}$ from the adjacent smaller element $(h\text{-}1)$th S_{h-1}
S_h	The h^{th} element in array $\mathbf{S_Q}$
S_{h-1}	The $(h\text{-}1)^{th}$ element in array $\mathbf{S_Q}$
$\mathbf{B}$	Auxiliary matrix that is obtained during the rejection process
n_{si}	Quantity of elements that are rejected. This quantity equals the difference N_{TRN}-$N_{max,TRN}$
T	Logical truth value
F	Logical false value
$N_{mim,4D}$	Bottom value for the size of Damage Diagnostic Decision Dataset
N_{4D}	Size of the Damage Diagnostic Decision Dataset
$N_{max,tst}$	Maximum allowable size of the testing dataset
N_{trn}	Size of the training dataset

$\mathbf{p_{o,3D}}$	Load amplitude array in the Damage Diagnostic Decision Dataset
$\mathbf{\omega_{o,4D}}$	Load frequency array in the Damage Diagnostic Decision Dataset
median	A MatLab function that calculates the median value of an array
IQR	A MatLab function that returns interquartile range of an array. The interquantile range is defined as difference between the third and the first quartile.
ε	Tolerance for the data diversity formulas
range ($[p_{o,min}, p_{o,max}]$)	Service range for the potential load amplitude values
range ($[\omega_{o,min},\omega_{o,max}]$)	Service range for the potential load frequency values

1. INTRODUCTION

This thesis concerns the design of an algorithm that is capable to detect structural damage in civil infrastructure bridges. The algorithm, which will be dubbed Damage Diagnostics System throughout the thesis, is the software component of a broader Bridge Health Monitoring System. This broader system integrates software and hardware, such as sensors and data acquisition components.

The material of the first section is divided in three subsections. Subsection 1.1 lists the general features of the Damage Diagnostic System and it discusses the research motivation. The same subsection justifies why this algorithmic solution is well suited for the damage diagnosis problem. In Subsection 1.2, the origins for the inspiration of the system are traced into biological and man-made systems. The final Subsection 1.3 is an overview of how the study is organized in the sections to follow.

1.1. RESEARCH OVERVIEW AND RESEARCH MOTIVATION

The rationale for the Structural Damage Diagnosis is based on the principle of the structural vibration testing. The Health Monitoring System captures the vibration signals, as the bridge responds to excitation from various sources. The purpose of the Diagnostic System is to extract information from the vibration signals concerning the damage condition of the bridge. This system will identify and quantify the damage, by examining the shifts in the vibration signature. This can be performed with a comparison between the actual vibration signal and the vibration behavior of the undamaged bridge.

There are two options to build the vibration model of the undamaged structure. The first option is to develop an analytical vibration model of the structure, based on theoretical assumptions of the bridge physical parameters, namely the mass, the stiffness and the damping. The other alternative is to create the model based on recorded vibration signals from the bridge that is characterized as undamaged. Recording the signals can be done at any instance during the bridge service life. At that instance, even though the bridge might be found to be undamaged after an inspection, it is very possible that there

is a deviation between the actual bridge physical parameters and the theoretical values. As for example, the damping might be different due to micro-cracks. These micro cracks that are developed to a limited degree.

These two models are not the same, because the analytical one is based on theoretical assumptions of the bridge physical parameters, while the second model is based on the actual state of the structure during an instance of the bridge service life.

However, because the vibration response of a bridge depends on a multitude of agents and parameters, it is not practical to build an analytical model for an existing bridge. For this reason, in this thesis, the Damage Diagnosis is based on a non-parametric vibration model of the undamaged bridge that is created by the Neuro-Fuzzy Networks.

These adaptive algorithms are suitable tools for the vibration-based diagnosis, because they satisfy its requirements, such as the need for autonomy, the dealing with non-linear functions, and the processing of incomplete or noisy data. Nevertheless, the Neuro-Fuzzy Networks face several hurdles, as for example the lack of generalization.

Because the Neuro-Fuzzy Nets are data-driven algorithms, their performance depends on the training datasets. In addition, the Neural Nets will provide good results, only if the testing datasets are somehow relevant to the training dataset. The manual preprocessing for collecting proper data is an additional difficulty that reduces the Damage Diagnostic System autonomy. But most of all, the reliability of the system is of great importance, since it arrives at vital decisions concerning the bridge safety and operation. Any compromise could increase the risk for human lives sacrifices or it could lead to financial losses by taking unnecessary actions, be that a bridge shutdown, or an ordered bridge inspection.

So, as the overall performance of the Damage Diagnostic System should be superior and trustworthy, this thesis introduces three techniques that attempt to improve the use of the supervised learning algorithms.

The first novel procedure aims to calibrate the Neuro-Fuzzy Networks and to remove the networks prediction error. The two other techniques intend to collect the proper training and testing sets, respectively. Both techniques aim to improve the performance of the intelligent algorithms.

This thesis is a stand-alone document, but all readers, who are interested in a deeper analysis of the subject, can refer to a second manuscript, which is a part of an extended research program for developing a Bridge Damage Diagnostic System.

The second document is the currently unpublished Master of Science thesis in Civil Engineering that will be presented to the faculty of University of Missouri-Rolla by D. Danilatos (2008). That thesis by D. Danilatos (2008) includes a detailed model of the bridge under the impact of moving loads, the derivation of the diagnostic formulas, the creation of the fuzzy rules, and the analysis of the Neuro-Fuzzy Architectures. The manuscript is rounded off with the simulation and the analysis of the fundamental Damage Diagnostic System.

From the other part, this thesis in Engineering Management introduces three advanced supplementary techniques to enhance the Diagnostic System's performance. These three techniques give the opportunity not only to design a hybrid diagnostic system but also to suggest improvements and innovations for the Neuro-Fuzzy Networks, in general. In this thesis, the interchangeable terms Structural Damage Diagnostic System or Structural Damage Diagnostic Algorithm or simply Damage Diagnostics refer to the subject of this thesis.

The next subsection discusses the biological inspiration for the Damage Diagnostic Systems.

1.2. BIOLOGICAL INSPIRATION AND INTERDISCIPLINARY INFLUENCE

While from the one part, scientists devote themselves to discover the laws of the nature; from the other part, engineers keep an eye open on the natural world, groping for inspiration. Numerous engineering novelties track their origins into biological organisms. Mechanical inventions, like the airplane and the robots, as well as computational tools, like the Artificial Neural Networks and the Genetic Algorithms follow examples of the Nature.

This subsection shows that the Structural Health Monitoring Systems are nature-inspired inventions, as well. The functions of an ambitious Monitoring System are

similar to those performed by the human nervous system. A naive description of the biological counterpart will illustrate the parallelism. When nociceptive nerves in the skin, are activated by stimulus, they send signals through the spinal cord to the brain. Processing of the information is translated to appropriate perception or painful emotions. Various stimuli, such as mechanical, chemical, thermal, can be detected and evaluated. If damage is identified, pain will act as a warning alarm and a signal for defensive reaction will be sent back to the muscles. The function and the abilities of the human nervous system are much more complex in reality. Nevertheless, the above short representation was adequate to conceptualize how and what a Bridge Health Monitoring System should be able to perform.

The development of the Neuro-Computing algorithms was inspired by concepts and ideas from various scientific fields, like for example Biology, Linguistics, and Neurophysiology. New fields of Neuro-Computing studies emerged from the mathematical formulation of scientific concepts. The Artificial Neural Networks, which took birth from the biological studies of brain and vision, and the Genetic Algorithm, which were evolved from the biological theory of evolution, are two characteristic examples to mention.

However, today most fields of study in Neuro-Computing are well established, so there is little space left to propose innovative algorithms. As a case in point, all inspiring concepts from Biology seem to have been already transfused into the corps of Intelligent Algorithms. Sometimes new proposed Neural Networks incorporate ideas, which although they look novel, they have little practical applicability. Furthermore, the performance of these networks is inferior when compared to the classic backpropagation network.

As the approach to scientific areas, which are traditionally related with Neuro-Computing, is exhausted, the researchers might have to search new grounds for inspiration. This thesis gets inspiration from the area of the Cognitive Psychology, in order to introduce a reductionistic model, which combines the Neuro-Fuzzy System with novel features.

Inspiration from biological structures is productive; however, since the old days of Renaissance, the unsuccessful efforts of Leonardo da Vinci to imitate birds, by

designing a flying machine with movable wings, reminds us a lesson. Biomimicry and anthropomorphic engineering designs, which slavishly ape nature, as likely as not doom to failure. Contrarily, research that is inspired by the natural laws is more efficient, as it has the potential to reveal new patterns and to develop original applications.

1.3. SECTIONS ORGANIZATION

The thesis is organized in six sections. The next section reviews on the past research that concerns the Structural Damage Diagnosis, by involving soft computing techniques. In addition, the Section 2 mentions fundamental concepts from the field of the Cognitive Psychology. These ideas will provide us the raw material for inspiration in the design of novel Smart Computing Systems, later in the next section. Moreover, Section 2 underscores what have not covered in the previous works and what the study's needs are.

Section 3 describes the model architecture for the proposed Damage Diagnostics System. Section 4 presents a simulation experiment in order to illustrate the material of the preceding section. Section 5 makes available the findings of the damage detection procedure that is tested on different simulated scenarios. Finally, Section 6 summarizes the research findings and presents the conclusions.

2. LITERATURE REVIEW

2.1. INTRODUCTION

This section reviews previous research in the area of the Structural Damage Detection. In parallel, this section draws attention to the points that require improvements.

The material is organized as follows. Subsection 2.2 reviews published papers that concern structural diagnosis, by using Intelligent Learning Algorithms. After summarizing and assessing the previous accomplishments, Subsection 2.3 discusses some commonly known hurdles that are associated with the use of the Adaptive Networks. The thesis intends to fix these problems. Subsection 2.4 provides a short introduction in the concepts of Cognitive Psychology. These concepts provide the inspiration for building the Neuro-Computing model architecture for damage diagnosis, to be presented in the next Section 3.

2.2. PREVIOUS RESEARCH FOR HEALTH MONITORING SYSTEMS

This subsection reviews the previous research efforts in performing Structural Damage Detection, using Intelligent Learning Algorithms. Taking into consideration the fact that this research area enlarges rapidly, the listing is unfortunately partial, and it is restricted to a limited number of representative papers.

In the first reviewed paper, H. - G. Herrmann and J. Streng (1997) applied a feed-forward Neural Network to identify damage on a planar statically determinate truss structure, composed by six rods. The Artificial Neural Network (ANN) consisted of six input and output neurons, which were intervened by two hidden layers, each having twelve units. The authors proposed a technique to enhance the network's training and generalization, using pre-processing of the data by dimensional analysis, according to the Pi-theorem. All data were generated by finite element analysis software. Inputs consisted of nodal displacements in two directions, when outputs were the actual to nominal stiffness ratios of the rods. The Optimal Brain Surgeon method by B. Hassibi et

al. (1992), which was incorporated, reduced the number of the hidden units, of the interconnections, and of the test error.

The authors did not vary the static force applied on the truss, which might be seen as a limitation in practical applications. Furthermore, an additional limitation was that the structure of the ANN required the number of the recorded displacements equaled to the number of the output structural integrity coefficients.

Masri et al. (2000) used a multilayer feedforward network to map the excitation force, measured displacement, and velocity of a non-linear dynamic system to the system's acceleration. However, more useful was proved the inverse modeling from the response to the excitation, which was also investigated and put into practice for damage detection. The input data, which fed into the Neural Network, were experimentally recorded accelerations and white-noise force excitation. Outputs were numerically integrated velocity and displacements. The ANN had a 9-15-10-4 topology and incorporated an adaptive random search technique (ARS), to deal with high-order systems of many parameters. The hyperbolic tangent was used as activation function. The Neural Network had been trained with experimental vibrational data of an undamaged mechanical system, so it was able to identify the same system under damaged state, within a norm error ratio approximately 10-15 %. The authors evaluated the network's performance using the RMS error, to compare between the predicted and the recorded data. The greater was the damage in the mechanical system, the greater was the difficulty experienced by the network to predict the response. Therefore, statistical parameters, like the dimensional standard deviation ratio were employed to evaluate damage in the structure. However, the authors pointed out that such damage indices might not indicate structural damage in quantitative, unique way, because the Neural Network used different starting weights. The following paper suggested a novel procedure to overcome the difficulty.

B. Zu and Z. Wu (2002) employed two Neural Networks to perform health monitoring on a four-story frame structure, excited by earthquake ground shaking. The two networks had the three-layer architecture, trained by backpropagation, but they served different purposes. The first Neural Network was able to predict the dynamic response of the healthy building structure to various seismic excitations. To achieve the

task, the network was trained with the values of displacement, velocity, and acceleration, undergone by each floor, at time step k. The output was the story displacement, at the next time step k+1. The training process took 10000 epochs. The neurons of the hidden layer were twice the number of the input neurons. To evaluate damage, the relative root mean square (RRMS) error was defined. The RRMS error correlated the tested value of displacement with the output of the Neural Network. The authors proved that this damage index did not depended on the seismic excitation, but it corresponded to the structure's stiffness. The RRMS error of the first Neural Network was subsequently used as input of the next network. The output of the second Neural Network was the stiffness of each story of the damaged structure. The authors claimed that by coupling the pair of Neural Networks, created a parametric identification strategy.

H. Luo and S. Hanagud (1997) developed a new Neuro-Fuzzy system, which was based on the steepest descent algorithm. It is well known that this variation of back propagation, besides it has low learning speed; it is apt to get trapped in local minima of the error surface. The authors suggest two procedures to improve the training performance. First, in order to avoid stopping of the algorithm in local minima, the learning rate was not only controlled by the error function but also by the error change. Secondly, they put into practice a fuzzy controller that derived the learning rate. The above-described Neuro-Fuzzy concept was able to detect delaminations and stiffness losses in laminate beam specimens.

Y. Q. Ni et al. (2002) used a multilayer perceptron (MPL), where the mapping from input to output patterns was done using auto-association. Two kinds of inputs were fed into the networks, in order to obtain different results: measured modal frequencies for damage identification and calculated modal flexibility for damage localization. In all cases, the output was a vector of statistical parameters of the input set. The evaluation of the damage was based on novelty indices, representing undamaged and damaged states. All the node structures that were employed had the following common characteristics, full symmetry of the network structure, equal number of the input and output nodes, two hidden layers with the same number of neurons, and fewer nodes in the hidden layer than in the external ones. The authors evaluated their method by using data experimentally

collected from three cable-supported bridges, which serve the traffic in the new international airport of Hong-Kong.

C. R. Farrar et al. (2002) underlined the importance to normalize vibration measurements used for the Health Monitoring of structures. The authors mentioned the following three normalization procedures. The first one was performed by subtracting the mean value of a vibration data series from the signal to eliminate DC offsets. The second one was done by dividing by the standard deviation of the measured time history. The scope was to normalize the varying amplitudes. The third procedure was the normalization of the measured vibration signal by the excitation input. In the case of a linear structure, the normalized signal became no longer related to the excitation.

However, apart from the primary measured excitation source, the structural response is also the result of a multitude of factors. In the case that measurements of the various operational and environmental conditions were not available, the authors suggested the use of the auto-associative Neural Network, which was formed by two feed-forward networks, serially connected. The researchers compiled a supervised network which was trained in a way that the networks output was related to the networks input. The objective was to perform data reduction and cleansing. The output values would be related with the measured primary source of system excitation, revealing the influence of the unmeasured secondary environmental parameters. Therefore, the proposed technique was able to detect vibrational changes, due to damage and not due to the variability of the environmental conditions. Because in investigated complex systems, the number of the external operational and environmental sources was unknown, the authors faced difficulties to define the dimensions of hidden layers in their network. In addition, another important drawback of the presented method was that the algorithm might disregard cases, where a damaged structure has the same vibration signature as a healthy one, under particular external conditions.

H. W. Shenton III and X. Hu (2001) proposed a method for determining the location and severity of damage in a clamped-clamped beam. The authors claimed that their technique could overcome several disadvantages of damage detection methods, which had been presented in the literature. From the one part, it is not always feasible or practical to meet the requirements of static methods: applying concentrated loads on large

structures, creating multiple load cases, and measuring the absolute deformation. From the other part, two problems of the dynamic techniques were solved; the difficulty to excite large civil structures to a sufficient level and the interference of environmental variable factors. The method by H. W. Shenton III and X. Hu was based on the principle of redistribution of dead load stresses due to the presence of damage and used measurements of strains, slopes, or displacements. The methodology was demonstrated with a simulated clamped-clamped beam and the authors believed that it has the potential to find application on large civil structures. The damage detection scheme was a constrained optimization problem with the objective function defined as the absolute error between measured and analytical strains at three locations of the beam. Unknown parameters were the damage location, length, and severity. A genetic algorithm was implemented in order to solve the optimization problem. The chromosome vector was encoded in floating point format. New chromosomes were created either by crossover using convex arithmetical operators and a rate of 0.5, or by dynamic mutation, with a rate of 0.3 and a degree of non-uniformity equal to 2. The authors were able to identify different severities of damage in alternate locations, even in the presence of noise. The genetic algorithm was also successful, when was tested with a false-positive case scenario. However, the drawback of the method was that it could not detect damage at the particular locations of the inflection points, where the strains were zero.

L. Meyyappan et al. (2003) performed off-line analysis on vibration data that were monitored from a steel truss bridge. During a controlled experiment, a vehicle driving at various speeds excited the structure. Two different analysis tools were used for damage detection. In both cases, the dimensionality of the vibration data was reduced, by selecting the peak values of the power spectrum as the characteristic feature to be analyzed. The first detection approach was based on the empirical assumption that the ratio between the peak values of the power spectrum at two different sampling locations is constant, and independent of the vehicle speed. Any discrepancy on the above mentioned ratio might indicate the presence and the location of damage. With the help of the Fuzzy C-means technique, the investigated modal values were classified into clusters. Then the developed fuzzy logic decision system identified damage, by comparing the

clusters of the model values with the clusters of an undamaged structure. The derivation of the empirical assumption was not provided.

The second damage detection approach, which was employed by L. Meyyappan et al. (2003), the Backpropagation Network with Levenberg-Marquardt method in order to model the relationship between the vehicle speeds and the power spectrum values. The trained Neural Network was capable to provide the reference vibration for the undamaged structure. This network had fifteen neurons in the input, in the hidden, and in the output layers. The networks input was the vehicle speed, the networks output was the peak power spectrum value. Different ANNs, which had the same architecture, were used for different sampling locations. In order to detect damage, the recorded vibration was compared with the reference undamaged vibration that is predicted by the ANN. This learning algorithm was used for damage detection, but it did not investigate the damage localization and quantification problem.

H. Adeli and X. Jiang (2006) developed a nonparametric system identification model. The identification is done using the Nonlinear AutoRegressive Moving Average with eXogenous inputs (NARMAX) to map the nonlinear relationship between the past observations and the future bridge response output. The first step in signal processing was the noise removal from the vibration signals, using the Wavelet Packet Transform Method. The reconstructed state space concept from the chaos theory was employed in order to prepare the input vectors for the NARMAX approach. The false nearest neighbor method was used to find the optimum dimensions for the NARMAX input space, which included the past bridge inputs and the past bridge outputs. The coefficients of the NARMAX were estimated by a hybrid Neural Network that incorporated several computing concepts. Because this was a dynamic time delay Neural Network, it was capable to memorize the past of the time series sensor data. The network's recurrent feedback topology consisted of an input, of a hidden and of an output layer. The activation function in the hidden layer combined fuzzy logic and decomposition that was based on the Mexican hat wavelet. The wavelets decomposition, which was the second application of wavelets in that research, facilitated the vibration data analysis by identifying nonlinearities in both the frequency and the time domains. Also, the wavelets represented the discontinuities in the vibration signals. In order to avoid the shortcoming

of the wavelets that might amplify local imprecision in the training data, the fuzzy logic was used. Thus, the data were partitioned into fuzzy clustered, using the fuzzy C-means algorithm. The modified Gram-Schmidt algorithm selected only the wavelets that best approximated the measured data and it eliminated all the rest wavelets. The number of the nodes in the hidden layer was further reduced by the Akaine's final prediction error criterion. The Levenberg-Marquardt least-square algorithm estimated the parameters of the fuzzy Wavelet Neural Network. By testing this method on a five-story steel frame, the authors reported that the system identifications had a root mean squared sum of errors less than 11%. This identification method might find applications on the Structural Health Monitoring Systems, although the paper did not include such as examples.

Table 2.1 and Table 2.2 provide an overview of the papers that have been reviewed in this section. Most of these papers employed a particular network, namely the backpropagation. Being encouraged by the research applications of the Artificial Neural Networks and of the Genetic Algorithms in the field of the Health Monitoring Systems, this research program applies the promising Adaptive Neuro-Fuzzy Inference System (ANFIS), which has been developed by J.-S. R. Jang (1993). Applying the ANFIS for bridge damage detection is presented in the other thesis by Danilatos (2008), which is the second manuscript that includes the findings of this research program. That thesis demonstrates that the Neuro-Fuzzy Network has the potential to exhibit advantages over the intelligent algorithms that have been previously tested. Nevertheless, the Damage Diagnostic Algorithm takes advantage of the incorporated Neuro-Fuzzy Inference Systems, but also it inherits practical drawbacks from these embedded intelligent algorithms. The next subsection presents certain hurdles that are related with the training and the testing datasets of the learning algorithms. This thesis does not only deal with the damage diagnosis problem, but in parallel, it introduces methodologies that intend to solve practical drawbacks of the supervised learning algorithms, in general.

Table 2.1. Overview table of the research papers that are reviewed in Subsection 2.2 (First part)

Paper	Architecture	Inputs	Outputs	Data Derivation
H.-G. Herrmann and J. Streng (1997)	MLP[2] - Optimal Brain Surgeon	Nodal displacements	Actual to nominal stiffness ratios	Analytical - Finite element analysis
Masri et al. (2000)	MLP	Accelerations & Force excitation	Velocity & Displacement	Laboratory Experiment
B. Zu and Z. Wu (2002)	Two serially connected MLPs with backpropagation	1. Displacement, velocity & acceleration 2. RRMS[3] error of the first ANN[4]	1. Future Displacement 2. Stiffness	Laboratory Experiment
H. Luo and S. Hanagud (1997)	Backpropagation Steepest Descent Fuzzy controller	Modal Frequencies	Stiffness losses	Laboratory Experiment
Y. Q. Ni et al. (2002)	MPL with auto-association	Modal frequencies and modal flexibility	Statistical parameters of the input set	Bridge Structures

[2] MLP: Multi-layer perceptron
[3] RRMS: Relative root mean square
[4] ANN: Artificial Neural-Network

Table 2.2. Overview table of the research papers that are reviewed in Subsection 2.2 (Second Part)

Paper	**Architecture**	**Inputs**	**Outputs**	**Data Derivation**
C. R. Farrar et al. (2002)	Two serially connected auto-associative MLPs	Modal Frequencies	Modal Frequencies	Laboratory experiment
H. W. Shenton III and X. Hu (2001)	Genetic Algorithm	Strain, Slopes, Displacements	Damage location, size and severity	Analytical
Meyyappan, L, et al. (2003)	Fuzzy C-means technique, Backpropagation Network with Levenberg-Marquardt	Vehicle Speed	Peak Power Spectrum, Damage Detection	Experimental
Adeli, H., and Jiang, X. (2006)	Dynamic Time-Delay Neural Network, Wavelet, Fuzzy logic, reconstructed state space concept from chaos theory, Levenberg-Marquardt algorithm, et al.	Acceleration, Excitation	Acceleration, Damage Detection	Experimental

2.3. KNOWN PROBLEMS WITH THE NEURO-FUZZY NETWORKS

Since the Adaptive Neuro-Fuzzy Inference System involves supervised learning from data, the prediction accuracy and the network performance depend on the training dataset. There are huge variations in "trainability" between different training subjects. K. Hornik, et al. (1989) demonstrated that the multilayer feedforward networks are universal approximators of any mathematical function. This commonly accepted property of the multilayer networks is valid for the ANFIS, as well. However, the theoretical capability of the learning networks to approximate any function presupposes the existence of an appropriate training dataset, as the lever of Archimedes is supposed to move the whole world, given a fixed fulcrum[5]. In practice, the main obstruction for attaining the goal of the universal approximation is the difficulty to obtain éproperé and sufficient training data. In the following lines, the discussion is about which properties of the training datasets influent the performance of the Neuro-Fuzzy Network. These characteristic properties are the size, dispersion, and comprehensiveness.

The first characteristic to be discussed is the training dataset size. For practical considerations, the checking and the testing datasets are equal in size with the training dataset. Therefore, growing the training set increases not only the training time, but the response speed of algorithm as well. By keeping the sets as small as possible, there is economy in computing resources and time. However, the influence of the decreased datasets on the learning quality might be degrading. Contrarily, the probability for a bigger dataset to include representative and diverse data is higher. In the search for the ideal size, it is important to consider the following matters. Following a general thumb of rule, it is advisable that the training datasets size is greater than the number of the ANFIS parameters. It has been showed that applying this rule improves the learning process. However, it is important to mention that the data reduction should not be done in the expense of the datasets dispersion and comprehensiveness. These two training datasets characteristics influence the ANFIS performance, as it is discussed below.

---

[5] To underline the theoretically unlimited mechanical advantage of levering, the great Greek engineer Archimedes (287–203 B.C.), once said éGive me a fulcrum point to stand and I will move the whole worldé. See the Columbia World of Quotations (1996).

The learning process of ANFIS is based on a backpropagation network, which is notorious for its problem with the lack of generalization. The system might face difficulties with the generalization due to several causes.

A training dataset that includes well distributed elements, which cover comprehensively the data space under consideration, contributes to avoid the common problem with the lack of generalization.

The common difficulty with the generalization is faced when testing data are outside the range of the training dataset. In this problem, the Neuro-Fuzzy Systems fails to provide successful predictions for the testing data, even if the training error had been very small. Therefore, the range of the potential values should be comprehensively represented in the training dataset, because the Neuro-Fuzzy algorithms perform some kind of sophisticated interpolation, among the training data. In addition, the training data should be well distributed along the range of the values that the system encounters potentially in practice.

In the following lines, the discussion is about how the training datasets characteristics influence the learning algorithms performance. This aspect is related with the testing datasets.

It is important that the learning algorithms exhibit good generalization. This means that the trained networks should be capable to predict never seen before inputs. However, to get satisfactory generalization, it is not enough to get the proper training datasets. It is needed also that the testing datasets should be drawn from the similar distributions as the training data. In addition, the testing data should lie within the training dataset range.

This subsection shows that the performance of the supervised learning networks requires that the training and the testing datasets possesses certain optimum characteristics. The common practice for obtaining these datasets is done by data preprocessing and manipulation of the raw data. To make the situation even more difficult to deal with, this data preprocessing is tedious and complicated, in most cases.

To avoid the aforementioned difficulties, this thesis introduces two automated sampling procedures, one for the training and one for the testing datasets. These techniques are presented in the Subsections 3.6 and 3.7.

Therefore, the selection of the training datasets size should balance two contrary goals; from the one part, the goal is to minimize the computing time and the computing resources and from the other part, it is desirable to keep the datasets diverse and comprehensive.

2.4. INSPIRATION FROM THE COGNITIVE PSYCHOLOGY

In this subsection, fundamental concepts and principles from the Cognitive Psychology are introduced briefly. Reviewing this material will provide the inspiration for the mathematical formulation of a hybrid cognitive model for damage diagnosis, which will be presented in the next section.

The Cognitive Psychology, which is the dominant field in the contemporary Psychology, studies the cognition, and in particular mental processes, like for example the memory, the perception, and the reasoning.

The most characteristic model in the Cognitive Psychology is the information processing approach, which was introduced by D. Broadbent (1958) and it was based and inspired by Computer Science studies. In the information-processing model, the analogs of the computer and of the software are the brain, and its mental processes, respectively. Apparently, the fields of the Cognitive Psychology and of the Neuro-Computing are interrelated, so it might be hard to distinguish whether the mentioned concepts have an origin in the former or in the latter scientific field. The transition of ideas between the two fields of study is highly beneficial for both parts.

To begin with, two basic terms in the Cognitive Psychology are introduced, namely the memory, and the intelligence.

The memory is related with the information processing mechanisms, like the information recording, storage, and classification, while the intelligence concerns processes that create links between the raw blocks of information. An important principle accepted by the cognitive psychologists is that the memory is selective and that the brain pays attention to stimuli that have particular interest. In this subsection, the presentation of the material from the Cognitive Psychology is done selectively as well, by

focusing on issues that interest us, even though this scientific field has become very wide, over the last years.

Studying the memory is a major issue in the Cognitive Psychology. Several theories have been proposed for modeling the memory. The stage theory, which was initially proposed by Atkinson and Schiffrin (1968), is one of the oldest models, that nevertheless it is still widely accepted. According to the stage theory, the information is processed in the three following stages: the sensory memory, the short-term memory, and the long-term memory. Another interesting concept is the forgetting mechanism, which pushes out surplus information in order to avoid cluttering of the short-term memory. Researchers have shown that learning is more efficient when it starts after forgetting has taken place. It is assumed that the short-term memory has limited capacity, while the long-term memory might be considered to have unlimited capacity, theoretically.

From the other part, the second Cognitive Psychology term to be discussed is the intelligence. The intelligence processes include the pattern recognition, the reasoning, among others. The reasoning, which is of particular interest herein, has two main subcategories; the inductive one and the deductive one. The former subcategory refers to the inference of a general conclusion from specific instances, while the latter is the inference of particular instances from a general function.

The memory and the intelligence are treated as two distinct functions, even if they are usually interrelated in such a close dependence that makes them hard to separate them. The operation of the intelligence is effected by the memory's function, because the intelligence provides links for data that are recalled from the memory. From the other part, in order to organize and to manage information, memory has to employ intelligent functions like for example the pattern recognition.

All the concepts and the terms, which have been presented in this subsection, provide us the inspiration for developing a cognitive model in Subsection 3.3. The coming section introduces the model architecture of the Damage Diagnostic System.

3. MODEL ARCHITECTURE

3.1. INTRODUCTION

In the previous section, the literature review gave indications that the bridge vibration signals reflect emerging structural damages. Based on this principle, the current diagnostic algorithm is designed to extract useful information from the recorded vibration signals, with the ultimate purpose to identify the presence and the degree of damage in structural bridges. The proposed methodology aims to overcome limitations of the past research efforts and to achieve a system with increased stability, robustness and efficiency. This section introduces the model architecture of the Damage Diagnostic Algorithm.

This section is structured in the following six subsections. Subsection 3.2 introduces the concept and the basic features of the Damage Diagnostic System. The Subsection 3.3 presents an alternate modeling of the Diagnostic System, which is inspired by theories of the Cognitive Psychology.

The remaining subsections present the components of the Damage Diagnostic Algorithm. The damage diagnostics algorithm engages two classes of Adaptive Neuro-Fuzzy Inference Systems (ANFIS), connected in series. Subsection 3.4 is devoted to the main characteristics of the ANFIS model. The next subsection is concerned with the datasets for the supervised learning algorithms. Finally, Subsection 3.6 studies an improvement procedure for sampling the training datasets and Subsection 3.7 develops a similar enhancement for the testing datasets.

3.2. DAMAGE DIAGNOSTICS SYSTEM MODEL

In this subsection, a detailed presentation of the Damage Diagnostic System for structural bridges is presented through illuminating figures. The proposed system is adapted either on a real-time scheme, or it can work off-line.

For demonstrating the diagnostic functioning, the following simple configuration is considered. The Health Monitoring system consists of two parts, the hardware, and the

software. The hardware includes sensors mounted on the structure, data acquisition systems, personal computers, and their peripherals. Optionally, the hardware might include communication lines and forced excitation devices.

Through the sensors, the Health Monitoring System monitors continuously three vibration parameters, namely the traffic bridge excitation p, the corresponding response acceleration $\ddot{z}$, and the deflection z. A simple test configuration for capturing the above parameters might be implemented to include an incorporated weight-in-motion roadway scale for the traffic loads, together with an accelerometer and a displacement instrument placed at the bridge mid-span. Any further details about the monitoring devices are not mentioned, because this thesis focuses on the algorithm development.

Two classes of Neuro-Fuzzy Networks are embodied in the Structural Damage Diagnostics Algorithm. The A-Class Neuro-Fuzzy Network maps the relationship between the bridge vibration response and the bridge excitation. From the other part, the B-Class estimates the prediction error of the A-Class network along its input space. The A-Class Neuro-Fuzzy Network is the main predictive algorithm for the Damage Diagnostic System. The output of the B-Class Network is used for calibrating the results of the first class Networks.

The pair of Networks, which occupies a fundamental position in the algorithm, is the driving power for prediction and diagnosis. Consequently, the Neuro-Fuzzy Networks determine main characteristics of the Damage Diagnostics model. Typical characteristics of the Neuro-Fuzzy Algorithms, like the distinctive and serial processes of training and testing, are also found in this model. Therefore, the Damage Diagnosis algorithm inherits the characteristic training and testing phases and the supervised learning procedures of the Networks.

Figure 3.1, Figure 3.2 and Figure 3.3 depict the three stages of the Damage Diagnosis in chronological order. Training the Neuro-Fuzzy Networks with undamaged data is taking place during the two first stages, while the third stage is devoted to the testing of the Networks. Each figure is detailed separately below.

As shown in Figure 3.1, in the first stage the A-Class Neuro-Fuzzy Networks is trained in a supervised way using training data that have been collected, during the undamaged bridge state. The detailed procedure for dataset formation will be presented

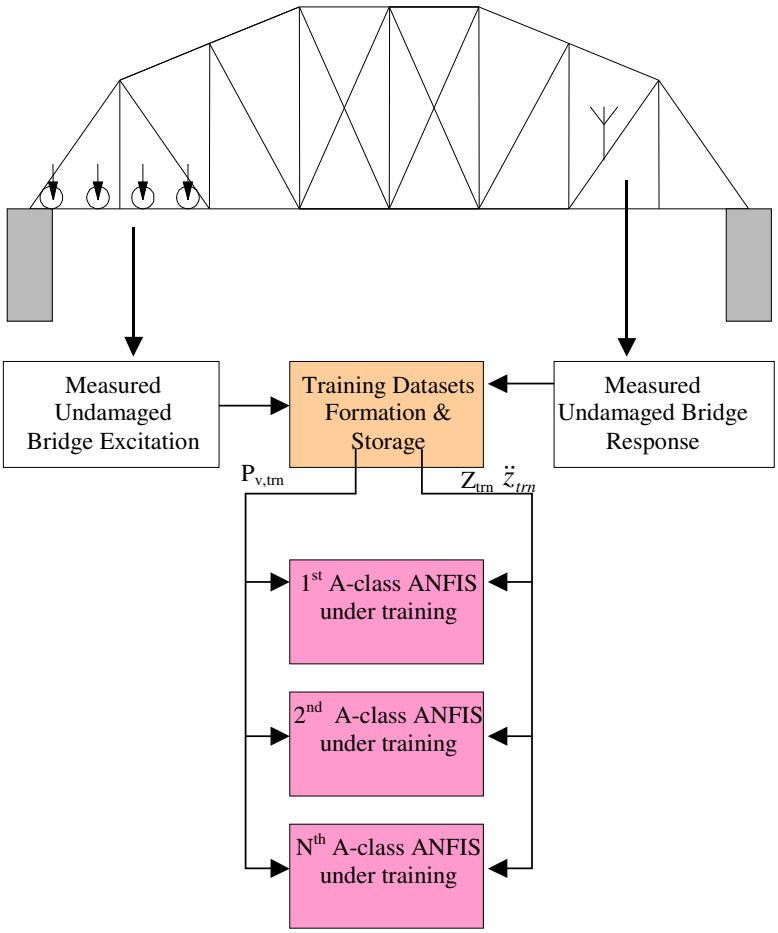

Figure 3.1. Training phase for the first Neuro-Fuzzy Architecture using data from the undamaged bridge

in Subsection 3.6. The training dataset assembles the networks inputs $\mathbf{z}_{trn}$, and $\ddot{\mathbf{z}}_{trn}$, along with the desired target outputs $\mathbf{p}_{trn}$. The subscript é*trn*é denotes the training data. The three arrays are clustered into F subsets, with respect to the different sampling instances i. Each one of the F subsets ($\mathbf{z}_{trn,i}$, $\ddot{\mathbf{z}}_{trn,i}$, and $\mathbf{p}_{trn,i}$) feeds a different Neuro-Fuzzy Network.

The two main processes, which are depicted in Figure 3.2, are the A-Class Neuro-Fuzzy Networks testing and the B-Class Network training. The sequence of the processes starts with the recall of the training inputs arrays $\mathbf{z}_{trn}$, and $\ddot{\mathbf{z}}_{trn}$. In this phase, these training arrays are used for testing the A-Class Networks. The ANFIS output is an

estimate of the undamaged bridge excitation $\mathbf{p}_{pred,trn}$ ($\mathbf{z}_{trn}$, $\ddot{\mathbf{z}}_{trn}$), which is a function of the vibration parameters $\mathbf{z}_{trn}$, $\ddot{\mathbf{z}}_{trn}$. Next, the average prediction error $e_{pred,trn}$ for the A-Class Neuro-Fuzzy Networks is calculated.

In the case that the bridge structure is linear, the systems prediction error $e_{pred,trn}$ provides an approximation of the predicted damage rate $\delta_{pred,trn.}$ But, during the testing phase of the Figure 3.2, the testing data come from an undamaged bridge, so the damage rate is zero. In that sense, when the predicted error $\varepsilon_{pred,trn}$ departs from zero, this is due

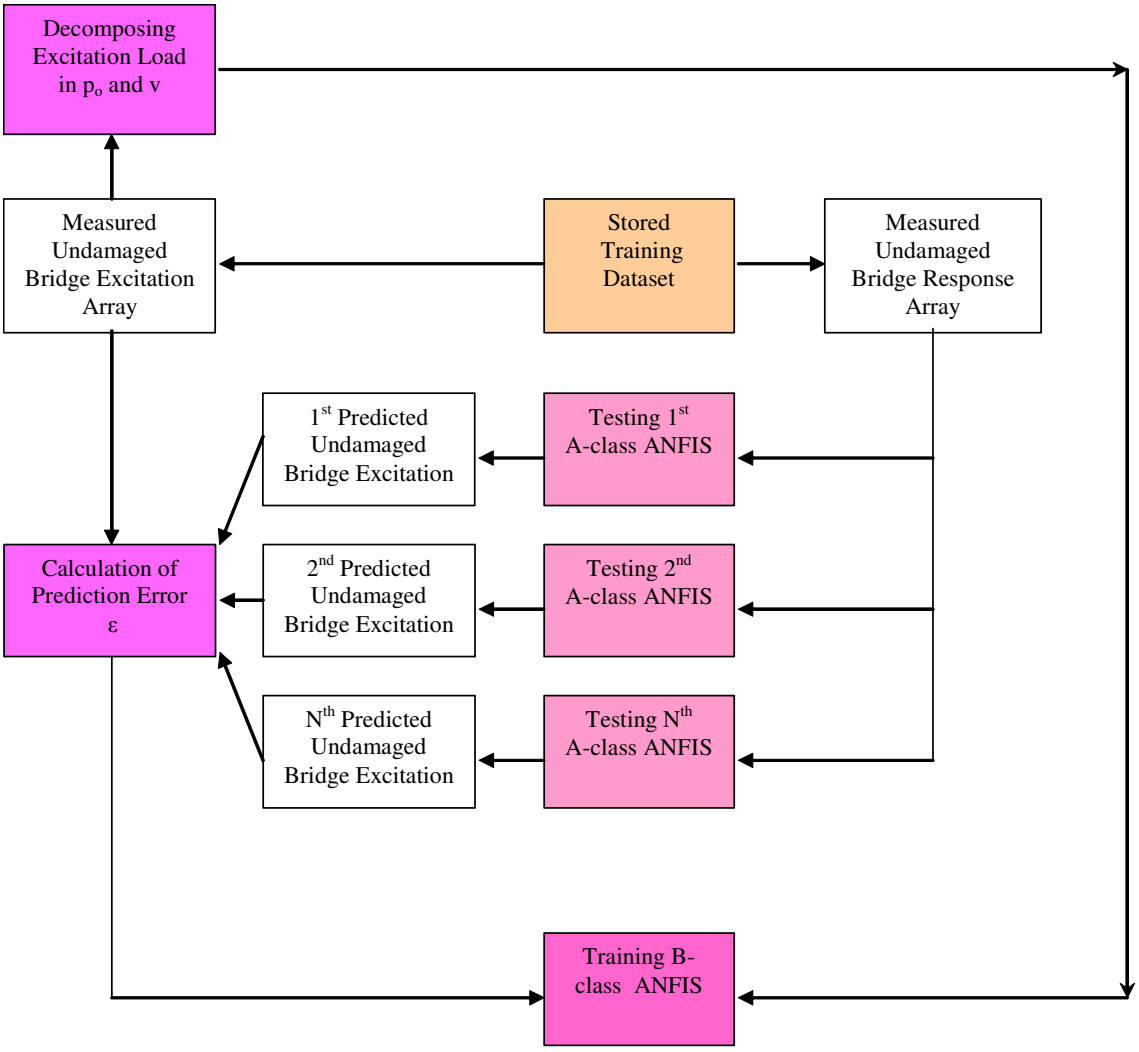

Figure 3.2. Testing phase of the A-Class Neuro-Fuzzy Architectures, by using the training data and training phase of the B-Class Neuro-Fuzzy Architecture

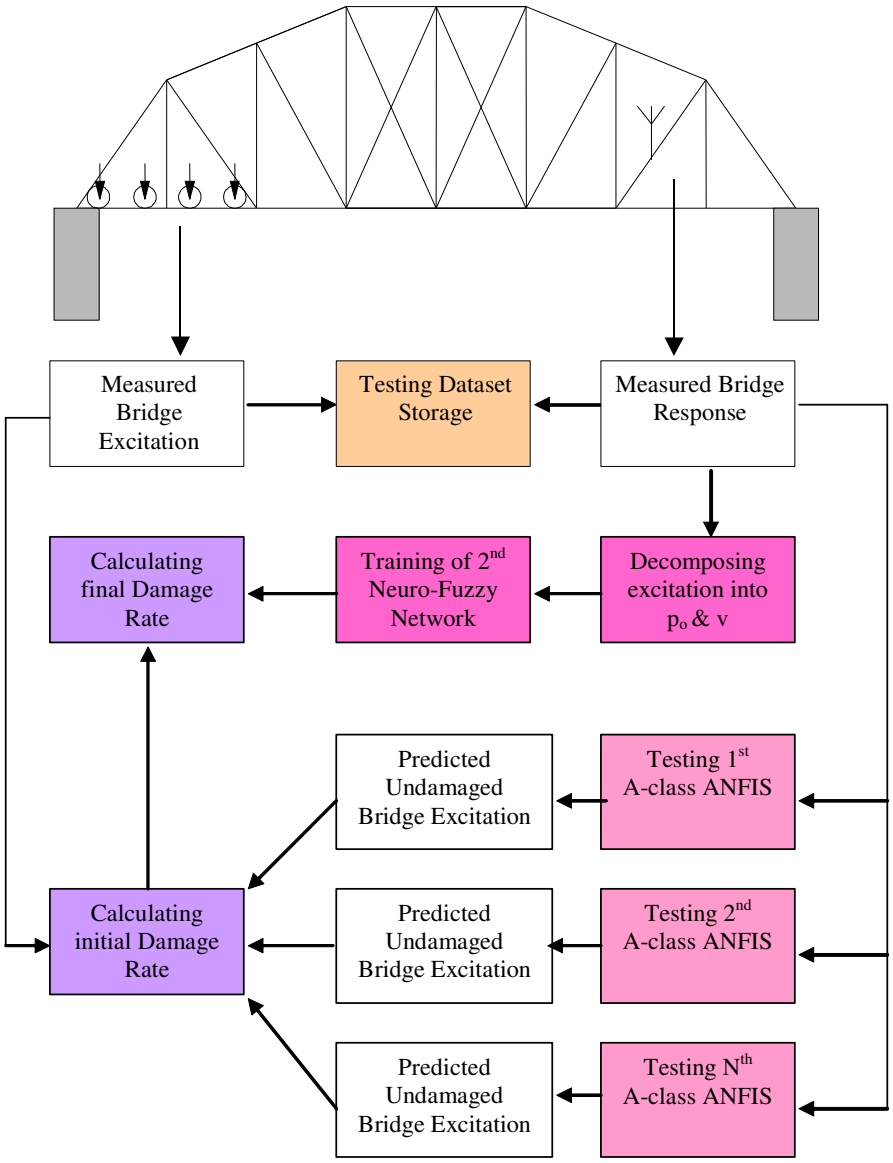

Figure 3.3. Testing both Neuro-Fuzzy Networks and damage detection

to systems training errors. Therefore, in the case of the undamaged bridge, the predicted error $e_{pred,trn}$ is not only a measure of the training performance, but also it indicates the confidence interval in the prediction of the bridge excitation $\mathbf{p}_{pred,trn}$.

Another block of the Figure 3.2 represents the decomposition of the measured excitation load $\mathbf{P}_v$ into two components, namely the vibration amplitude $\mathbf{p}_o$ and the vibration frequency $\boldsymbol{\omega}_o$. To form the training dataset for the B-Class Neuro-Fuzzy

Network, the two arrays $\mathbf{p}_o$, and $\boldsymbol{\omega}_o$ are set as inputs and also the corresponding prediction error array **e** is set as the target output. Figure 3.2 is rounded off with the block that represents the training phase for the B-Class Network.

Figure 3.3 is devoted to the damage detection and to the damage quantification, by employing the chain of the two classes of Neuro-Fuzzy Networks. In Figure 3.1 and Figure 3.2, the bridge data were from an undamaged bridge, but during the testing phase in Figure 3.3, the bridge is at an unknown damage state. The training of both classes of Networks has already been completed in the previous phases. In this third phase that is depicted in Figure 3.3, the system analyzes the vibration parameters z_{tst}, $\ddot{z}_{tst}$ and p_{tst} that are captured during the bridge service life.

The first process in Figure 3.3 is the formation of a testing dataset that includes enough samples for a confident and meaningful damage detecting decision. The detailed procedure for the formation of this decision dataset will be presented in Section 3.7.

The A-Class Network is presented with bridge kinetic responses, $\mathbf{z}_{tst}(t)$ and $\ddot{\mathbf{z}}_{tst}(t)$, in order to predict the excitation load $\mathbf{p}_{pred,tst}$. The predicted $\mathbf{p}_{pred,tst}$ is an imaginary excitation that would be applied to the bridge at the undamaged state, in order to produce the actual bridge responses $\mathbf{z}_{tst}(t)$ and $\ddot{\mathbf{z}}_{tst}(t)$.

The B-Class Network, which is fed with inputs p_o and ω_o outputs the prediction error $e_{pred,j}$. The prediction error will be used in order to adjust the first estimate of the damage rate δ_{pred}, and the corrected damage rate is obtained, by using the following formula:

$$\delta'_{pred,j} = \frac{\sqrt{\sum_{i=1}^{F}\{\frac{p_{v,j}(t_{i,j}) - p_{pred,j}(\ddot{z}(t_{i,j}), z(t_{i,j}))}{K \cdot z_j(t_{i,j})}\}^2}}{F} - \varepsilon_{pred,j}, \quad (1)$$

where $\delta'_{pred,j}$ is the corrected root-mean-square predicted damage rate that is calculated with samplings during the vehicle event j, K is the Stiffness Matrix and $\varepsilon_{pred,j}$ is the prediction error for vehicle event *j*, as it is estimated by the B-Class Neuro-Fuzzy Network.

For the derivation of formula (1), refer to D. Danilatos (2008). The damage rate, which is calculated through the above formula, corresponds to a single vehicle event. The final step includes the averaging of multiple vehicle events, in order to get results of increased confidence.

3.3. ALTERNATE MODEL FOR THE DAMAGE DIAGNOSTIC SYSTEM

The previous subsection introduced an initial model for the Damage Diagnostic System. This subsection presents a more complex and conceptual model, which stands in parallel to the previous one. Presenting various models of the system in progressively increasing complexity facilitates the understanding of this theory. The new model is inspired by Cognitive Psychology theories, which have been introduced in Subsection 2.4. The terms and the concepts from the Cognitive Psychology gain a different meaning here, as they are taken in a different context, and as a result, novel associations emerge.

The Damage Diagnostic model is presented in three sequential phases, namely the training datasets formation phase, the learning phase, and finally the deductive reasoning phase. The damage diagnosis is performed during the final reasoning phase; however, the two precedent phases are necessary for the system in order to attain its reasoning capability. The three phases are depicted individually in Figure 3.4, Figure 3.5, and Figure 3.6. In the following approach, the mental processes of the memory and of the reasoning are treated separately, as it is commonly done in the Cognitive Psychology treatises.

Figure 3.4 represents the mental processes for the training datasets formation phase. This phase includes the following three memory processes, namely the information preprocessing, the forgetting mechanism, the short-term memory function and the storage in the long-term memory. These memory processes, which are depicted in Figure 3.4, are analogous to the three stages of the memory model that was suggested by Atkinson and Schiffrin (1968). This model was mentioned in the Subsection 2.4.

As it can be seen in Figure 3.4, the sensory stimuli, which are captured by sensors that are mounted on the bridge, flow and get processed block by block, until the training

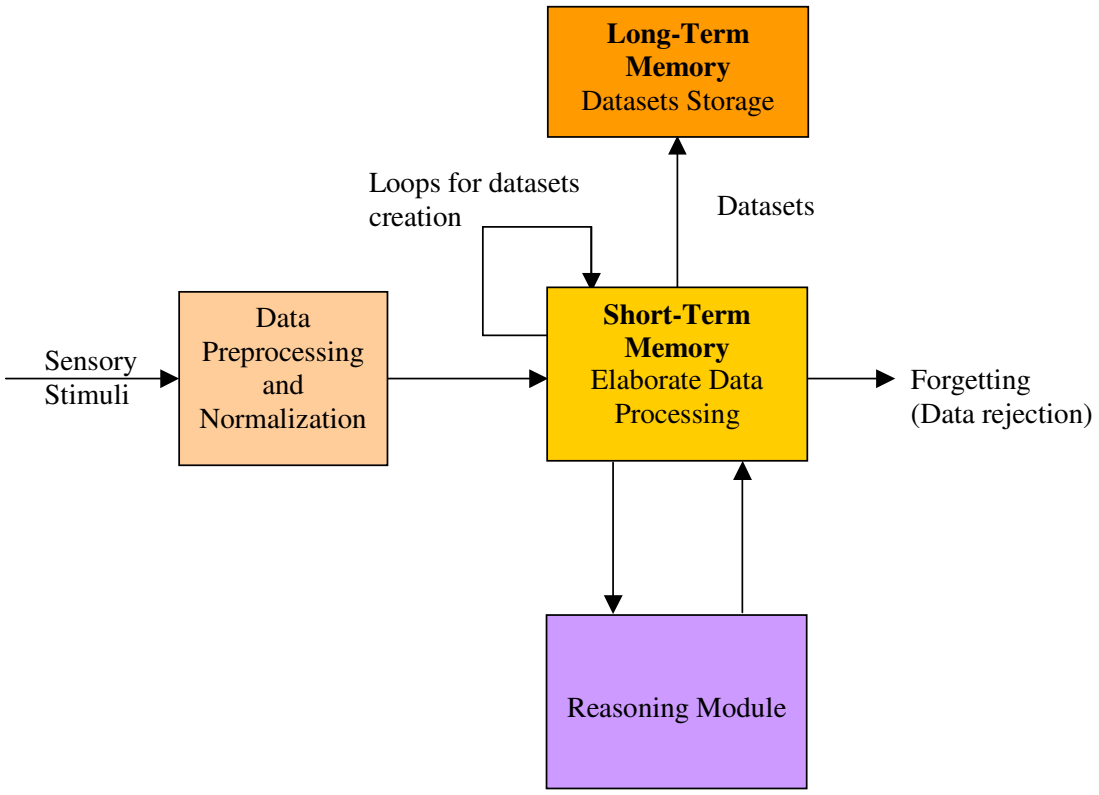

Figure 3.4. Memory processes and phases from the sensory data collection to the training datasets formation

datasets are formed. During this phase, the data are recorded from an undamaged bridge. The first memory module concerns the data preprocessing and normalization of the sensory stimuli. The second memory module concerns the elaborate information processing, which eventually ends with the training datasets creation. In collaboration with the forgetting and with the reasoning, this short memory block has the scope to collect a training set that includes representative data along the desired service spectrum. This procedure is iterative.

Subsection 2.4 mentioned that human brain learning becomes more efficient, when it follows a phase of forgetting. In addition, this subsection underscored that the

short-term memory has a limited capacity, while the long-term memory is theoretically unlimited. This modeling incorporates these two observations. In Figure 3.4, forgetting is the metaphor for the process of data rejection. Rejecting data of low importance is a part of the iterative procedures in order to create information dense training datasets. Data that do not meet the required standards are rejected, in order to free up space in the limited short-term memory. The data rejection pushes out of memory data that do not contribute new information, in order to keep the data that include new interesting features. Finally, the third memory module concerns the training data storage in the long-term memory.

In the scheme of Figure 3.4, the reasoning module simply supports the short-term memory, in order to evaluate the importance of the data and to facilitate the decision making for data rejection. The training datasets formation, which was depicted in Figure 3-4, will be found a detailed formulation in Subsection 3.6. The training datasets formation is necessary for both the A-Class and the B-Class Neuro-Fuzzy Architectures. Figure 3.5 depicts the learning phase processes. The first step in this figure concerns the training datasets that are retrieved from the long-term memory in order to feed the reasoning module. Reasoning means the inference of a general function from the particular cases that are included in the training datasets. In the case of training the A-Class Network, the sought-after general function is the relation between the inputs $\mathbf{z}$, and $\ddot{\mathbf{z}}$ and the target output $\mathbf{p}$. From the other part, in the case of training the B- Class Network, the sought-after general function is the relation between the two inputs p_o and ω_o, and the target output, which is the prediction error $e_{pred,j}$. In both classes of networks, the general functions are expressed as information about the trained Fuzzy Inference System (FIS). In Figure 3.5, the learning phase is rounded out with the long-term memory module that stores the FIS information.

Figure 3.6 presents a mental processing model for the Damage Diagnosis. At this phase, the bridge damage status is unknown. In this figure, two main stages are distinguished. The first stage, which includes the two top module blocks, is about the formation of the testing dataset, while the second stage, which is depicted in the three bottom blocks, concerns the damage diagnosis. The procedures are described in detail below. In the first module of Figure 3.6, the sensory data are pre-processed and

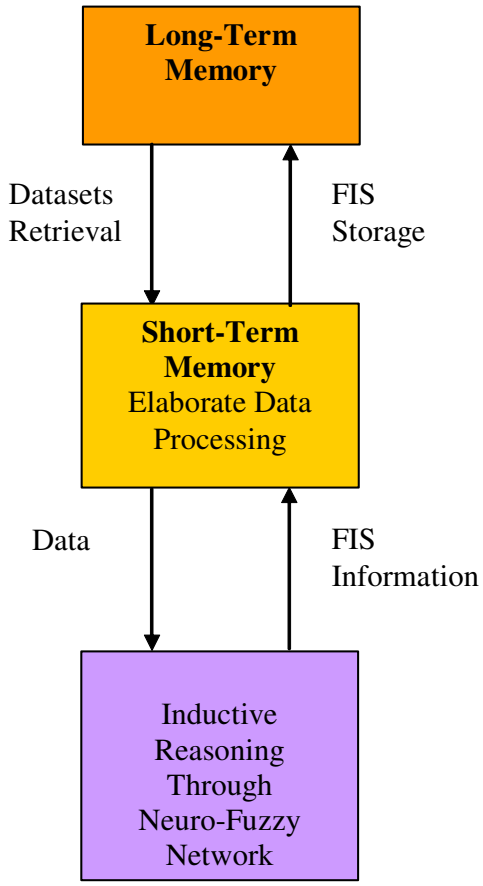

Figure 3.5 Learning by past cases

normalized. Then, in the next module of the short-term memory, through an iterative procedure, the selection of the testing data is done by considering those that are relevant to the previously collected training data. The learning algorithm will have a better performance, if the two datasets exhibit comparable statistical characteristics. The 4D method retains testing data that satisfy the above selection criterion. Otherwise the data are rejected (forgetting mechanism). This iterative procedure for creating the testing datasets is dubbed 4D in this thesis. The 4D method is treated in detail in Subsection 3.7. This procedure is similar to the iterative method for the training datasets, which was presented in Figure 3.4.

The next module in Figure 3.6 concerns the deductive reasoning through ANFIS. The measured vibration inputs are plugged into the previously derived general function,

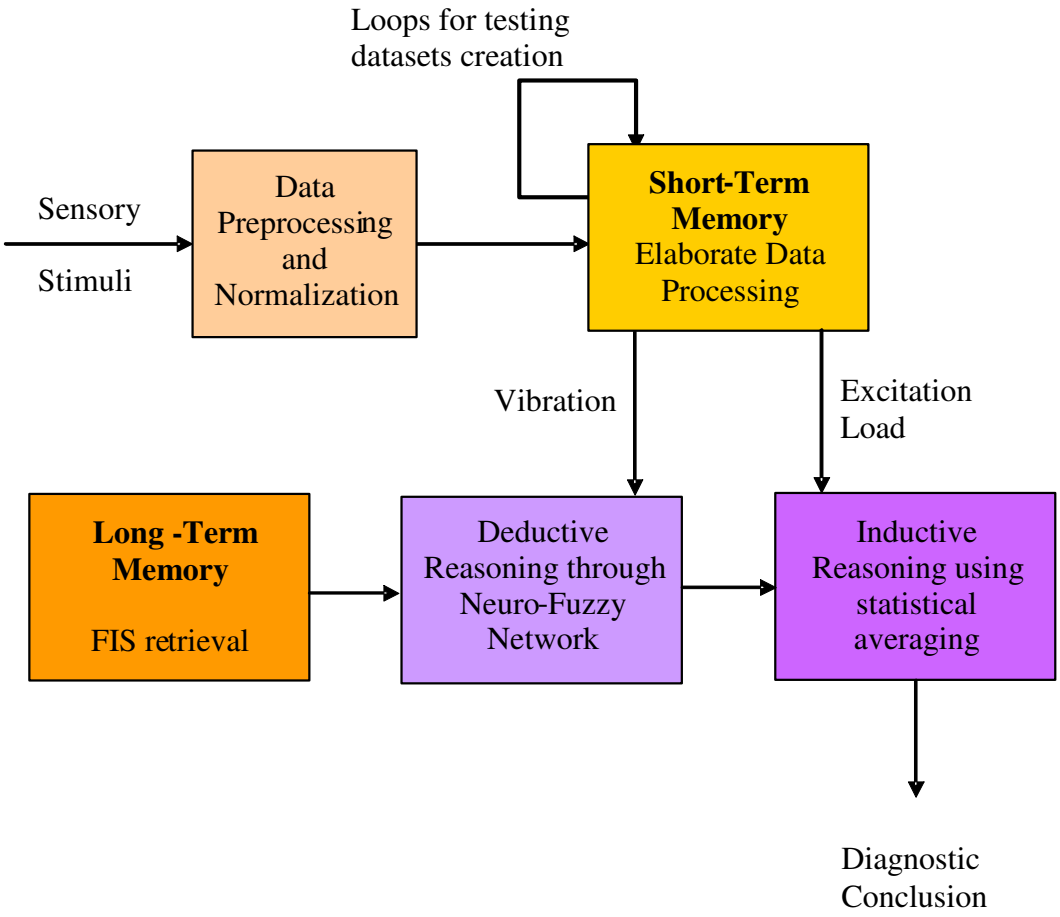

Figure 3.6 Damage detection in a mental processing model

in order to get an estimation of the equivalent excitation of the undamaged bridge. By comparing this estimated excitation with the actual excitation load, it is possible to conclude about the presence of damage. In the final reasoning module of Figure 3.6, the comparison between the measured and predicted excitations is repeated for all elements of the dataset, and the results are averaged, in order to extract the diagnostic conclusion.

This Subsection introduced an abstract model of the Damage Diagnostic System, by using Cognitive Psychology terms. From the one part, this model is an alternate version of the model that was presented in the previous section. From the other part, this model includes two novel components. These two novelties, which are related with the function of the short memory, are procedures for the formation of the training and of the

testing datasets. The short-term memory, which includes a forgetting mechanism, was modeled verbally and graphically in Figure 3.4 and in Figure 3.6. The mathematical formulation of the short-term memory for creating the training and the testing datasets will be presented in the Subsections 3.6 and 3.7, respectively.

The remaining subsections discuss the components of the Damage Diagnostic System, in detail.

3.4. SUPERVISED LEARNING ALGORITHMS

Subsection 3.2 mentioned that two classes of the Neuro-Fuzzy Networks are embedded in the Damage Diagnostic System. Each class serves a different purpose, but their architecture is the same in both cases.

ANFIS builds and analyzes a Fuzzy Inference System, whose fuzzy parameters are adjusted by a hybrid backpropagation network with least squares. The type of the employed Fuzzy Inference System is a first-order Sugeno-type system, which was proposed by T. Takagi and M. Sugeno (1985), and for that reason it was named after its two authors.

In this thesis, ANFIS is implemented by writing codes through the command line of the Fuzzy Logic Toolbox of MatLab (Fuzzy Logic Toolbox User's Guide (1999)). MathWorks, Inc produces the computer language for technical computing MatLab and its embedded toolboxes (MatLab, release 13).

3.5. DATASETS FORMAT AND CHARACTERISTICS

The Neuro-Fuzzy Networks are driven by sensory data captured from the bridge dynamic system. This subsection discusses how these data are organized in datasets.

The Neuro-Fuzzy System requires three types of datasets, namely the training, the checking, and the testing datasets. The first two types assemble data that are collected while the bridge is at the undamaged ('virgin') state. On the contrary, the testing dataset

includes records from undamaged states and from states at which the damage increases progressively.

The two first groups are used during the learning phase of the network for the validation of the structural model. During this learning phase, the Neuro-Fuzzy Network extracts the undamaged bridge model from the training data. The role of the checking dataset is to avoid learning over-fitting of the training data. From the other part, once the Neuro-Fuzzy Network is trained, the testing dataset validates the bridge structural model and verifies the recall ability of the Network.

At first, the discussion is about the size and about the characteristics of the datasets for the A-Class ANFIS. The three datasets for the A-Class ANFIS are multidimensional matrices, with a size of R-by-3-by-F. The amount of the rows R is not predetermined, but it depends on the iterative procedure for the training datasets collection. This iterative procedure will be the subject of the Subsection 3.6. The amount of the rows equals the number of the iterations, when the iterative procedure convergences. Each row of the multidimensional matrices assembles a different vehicle event. The three datasets have the form inputs-output. The inputs deflection and acceleration are arranged in the first and the second columns, respectively. From the other part, the third column includes the output excitation force.

The datasets for the B-Class Neuro-Fuzzy Networks are R-by-3 matrices. Again each row in these matrices assembles signals for a different vehicle event. The first column includes the moving load amplitude data; the second column assembles the load frequency data, while the third column contains the error e of the A-Class Network.

The coming two subsections introduce the two novel procedures that perform automatic preprocessing, in order to collect the training dataset and the testing set.

3.6. SAMPLING PROCEDURE FOR TRAINING DATASETS

3.6.1. Introduction. The proposed technique for improving the training datasets is dubbed MOJO in this thesis. This procedure, which is iterative in nature, performs automatic data preprocessing and data screening. MOJO process is remotely related with

the elaborate data processing in the short-term memory that was presented in Figure 3.4. The scope of the MOJO procedure is to address the problems that were mentioned in Subsection 2.3. Therefore, the method aims to create datasets with increased data dispersion, and with limited dataset size. These datasets should include representative values sampled in a wide enough spectrum.

The principle of the MOJO procedure is explained below. Suppose that a learning algorithm should be trained, so it is capable to recognize the patterns of a number of different objects. Collecting the highest possible number of training examples would make the training dataset too big to handle. For this way, the MOJO procedure assembles only a limited number of representative examples from each different category of objects. In this way, the training dataset contains only the essential information in a compact size.

The MOJO procedure is an iterative process that collects training data until the three following criteria are satisfied. The first two criteria concern dataset properties, namely the dataset size and the dispersion, while the third criterion measures the performance of the Adaptive Neuro-Fuzzy Inference System. The MOJO procedure is rounded off with a data rejection technique to remove data that prohibit the fast iteration of the algorithm.

Subsection 3.6.2 provides the details about setting up and selecting the convergence criteria for the MOJO procedure. Then, Subsection 3.6.3 explains the rejection technique. Finally, Subsection 3.6.4 describes the MOJO method through a general flowchart.

3.6.2. Convergence Criteria for the MOJO Procedure. In this subsection, the three convergence criteria for the MOJO procedure are formulated. These criteria concern the datasets size, the data dispersion, and the learning quality of the embedded Neuro-Fuzzy Systems.

The first criterion to be discussed concerns the A-Class training datasets size. The size N_{trn} of the training dataset should be kept between two boundary limits. It should not be bigger than the ceiling value $N_{max,trn}$ and not smaller than the bottom value $N_{min,trn}$.

$$N_{min,trn} \leq N_{trn} \leq N_{max,trn} \tag{2}$$

The boundary values are selected by taking into consideration the following factors. As a result, the ceiling value $N_{max,trn}$ depends on the available computing resources, but also it depends on the desired training and response time of the algorithm. The bottom value $N_{min,trn}$ depends on the network size, on the network topology and on the size of the largest input range $[z_{min}, z_{max}]$, or $[\ \ddot{z}_{min}\ ,\ \ddot{z}_{max}\ ]$, where z_{min}, $\ddot{z}_{min}$ are the minimum values that any elements in the deflection or acceleration arrays might take potentially, during the service life of the bridge. By analogy, the values z_{max} and $\ddot{z}_{max}$ are the maximum of the aforementioned arrays. Therefore, the bottom value $N_{min,trn}$ should be selected, in such a way that the training dataset contains a satisfactory number of exemplars.

The second criterion for the MOJO iterations concerns the training dataset dispersion. Before presenting the formulation for these criteria, the appropriate notation for the training datasets is introduced.

The trainings datasets for the A-Class ANFIS are triplets $(\mathbf{z}, \ddot{\mathbf{z}}, \mathbf{p})$ that include the inputs z and $\ddot{z}$, and the outputs p. Because the mathematical relationship between the two inputs (z and $\ddot{z}$) and the output p is defined uniquely, the data dispersion of the variable p is considered only. Let assume that the excitation force p(t) for each vehicle event is a sinusoidal function of a single frequency, so for simplicity each vehicle vibration signal is analyzed into two characteristic harmonic parameters, the amplitude p_o and the frequency ω_o. Therefore, the training data dispersion is converted into spreading out samples of the parameters p_o and ω_o. The following subsection introduces the methodology for spreading out these data.

Let suppose that the technical specifications of the vehicles that are currently in use in the country are known. Based on this information, the most severe loading p_{max}, or a combination of the spatial vehicle loadings $\{p_{max,1}, p_{max,2} \ldots, p_{max,n}\}$ for the bridge can be estimated. Consequently, the maximum amplitude $p_{o,max}$ and the maximum frequency $\omega_{o,max}$ can be calculated. In addition, the minimum values of the excitation force p_{min}, of the amplitude $p_{o,min}$ and of the frequency $\omega_{o,min}$ are zero or they are slightly higher than the value zero, as shown in the following formulas,

$$p_{\min} \approx 0 \quad , \tag{3}$$

$$p_{o,\min} \approx 0 \quad , \tag{4}$$

$$\omega_{o,\min} \approx 0 \quad . \tag{5}$$

Then, the interval ranges between the probable minimum and maximum values, $[p_{o,min}, p_{o,max}]$, $[\omega_{o,min}, \omega_{o,max}]$ are defined. Any random variable of p_o, or ω_o will fall in the above intervals and as a result, the associated probabilities are equal to one,

$$P_r(p_o \in [p_{o,min}, p_{o,max}])=1 \qquad \forall p_o \in \Omega_{p_o} \quad , \tag{6}$$

$$P_r(\omega_o \in [\omega_{o,min}, \omega_{o,max}])=1 \qquad \forall \omega_o \in \Omega_{\omega_o} \quad , \tag{7}$$

where P_r is the probability function, Ω_{p_o} is the sample space that includes all the potential values of p_o, and Ω_{ω_o} is the sample space that includes all the potential values of ω_o.

The ranges $[p_{o,min}, p_{o,max}]$ and $[\omega_{o,min}, \omega_{o,max}]$ are divided into a number of *s* segments that have equal ranges. Apparently, the width of each segment equals the one 1/*s* fraction of the total range. The dataset dispersion criteria are satisfied if all the *s* subsets contain the minimum desired number of data N_s, at least. In the case that the value N_s takes the value 1, the formulation of the dataset dispersion criteria is given below:

$$[(p_{o,\min} + \frac{p_{o,\max} - p_{o,\min}}{s} * a), (p_{o,\min} + \frac{p_{o,\max} - p_{o,\min}}{s} * (a+1))] \neq \emptyset, \ \forall a \in [1,2,...,s-1], \tag{8}$$

$$[(\omega_{o,\min} + \frac{\omega_{o,\max} - \omega_{o,\min}}{s} * a), (\omega_{o,\min} + \frac{\omega_{o,\max} - \omega_{o,\min}}{s} * (a+1))] \neq \emptyset, \ \forall a \in [1,2,...,s-1], \tag{9}$$

where α is a positive integer that is smaller than *s*.

The above two formulas concern the second convergence criterion for the MOJO procedure. In detail, Formula (8) concerns the dispersion of the load amplitude p_o, while the formula (9) assures the dispersion of the load frequency ω_o value.

The third criterion for the MOJO procedure concerns the learning quality of the A-Class Neuro-Fuzzy System. Four indices for the learning quality are defined below. The notation R is for the amount of the moving vehicles events in all datasets. Also, each event has a number of F measurements, during the time that the vehicle crosses the span. Then, for each row j in the datasets, there are two corresponding root-mean-square prediction errors $e_{j,trn}$ and $e_{j,chk}$ for the training and checking datasets, respectively. The subscript j indicates that the vehicle event takes the values j ∈ [1,…, R]. The values of the errors $e_{j,trn}$ and $e_{j,chk}$ are assembled in two sets, which are noted as $\{ e_{j,trn} \}$ and $\{ e_{j,chk} \}$. Errors $e_{j,trn}$ and $e_{j,chk}$ indicate the confidence interval for the systems prediction. In other words, the errors e_j are indicators of the networks capability in predicting the damage rate. The smaller the error *e* is, and the more the error *e* approaches to zero, the better the network training and predictability are. The two statistical parameters for the above two sets, namely the square-root-mean and the variance, are defined as the four indices for the learning quality of ANFIS. These four indices are calculated with data from the bridge at undamaged state. The indices for the learning quality consider the checking dataset as well, in order to cross-validate that the ANFIS avoids over-fitting the training data.

The following four inequalities provide the learning quality criteria that should be met:

$$\overline{e}_{trn} = \frac{\sum_{j=1}^{M} e_{j,trn}}{M} < e_{\lim,trn} \quad , \tag{10}$$

$$\sigma_{trn} = \sqrt{\frac{1}{M-1} * \sum_{j=1}^{M} (e_{j,trn} - \overline{e}_{trn})^2} < \sigma_{\lim,trn} \quad , \tag{11}$$

$$\overline{e}_{chk} = \frac{\sum_{j=1}^{M} e_{j,chk}}{M} < e_{\lim,chk} \quad , \tag{12}$$

$$\sigma_{chk} = \sqrt{\frac{1}{M-1} * \sum_{j=1}^{M} (e_{j,chk} - \overline{e}_{chk})^2} < \sigma_{\lim,chk} \quad , \tag{13}$$

where $\bar{e}_{trn}$ and σ_{trn} are the arithmetic mean and the variance of the errors e_j for the A-Class training dataset, respectively. The values $\bar{e}_{chk}$ and the σ_{chk} concern by analogy the A-Class ANFIS checking dataset. Finally, the $\bar{e}_{lim,trn}$ and the $\sigma_{lim,trn}$ are the imposed limits on the root-mean-square and on the variance of the training errors e_j, respectively. The $\bar{e}_{lim,chk}$ and the $\sigma_{lim,chk}$ are the analogue limits for the checking dataset. The above formulas map each dataset into two scalar values.

The inequalities in formulas (10) and (12) imply that the root-mean-square of the prediction errors should be smaller than the imposed limit $\bar{e}_{lim}$. From the other part, the inequalities in formulas (11) and (13) state that the variances are bounded by the imposed upper limit σ_{lim}. The smaller the variance is, the more the prediction errors will be concentrated around the mean. The above four criteria do not set boundary limits on separated error values, but on the two main statistical parameters of the errors set. Focusing on the statistical parameters provides a practical solution, that it is very helpful when dealing with complex and extended spaces.

3.6.3. Rejection Process. During the MOJO procedure, the rejection process will be activated, if the training dataset reaches the maximum size Nmax, but the two other MOJO criteria have not yet been converged. The rejection process is the subject of this subsection.

There are three variations of the rejection process. The type I rejection will be activated, if the dispersion criterion for the array $\mathbf{p_o}$ is not satisfied. This rejection focuses on the Euclidean distance between the elements in the $\mathbf{p_o}$ array. From the other part, the type II rejection concerns the array $\boldsymbol{\omega_o}$. Finally, the type III process rejects particles based on their Euclidean distance in both arrays $\mathbf{p_o}$ and $\boldsymbol{\omega_o}$. The type of the rejection III will be selected, if the dispersion criterion is not satisfied for both arrays $\mathbf{p_o}$ and $\boldsymbol{\omega_o}$, or the learning quality criteria are not satisfied. Otherwise, all the three types of rejections work fundamentally in the same way. The type I rejection is presented as the standard theme.

As a first step in the rejection procedure, the array p in the training data is replaced with the arrays of the characteristic harmonic parameters p_o and ω_o. In this way, the outcome is the matrix $\mathbf{A} = [\mathbf{z}\ \ddot{\mathbf{z}}\ \mathbf{p_o}\ \boldsymbol{\omega_o}]$. Next, the number of the superfluous data is

identified. Then, the superfluous data should be removed, in such way that the remaining set will be within the size limits. The criterion for selecting the rows (z $\ddot{z}$ p_o ω_o) that should be rejected is the Euclidean distance of the elements p_o or ω_o from the rest elements in the arrays $\mathbf{p_o}$ or $\boldsymbol{\omega_o}$, respectively. The elements of the rejected triplets are these that are located nearest to the other data. Therefore, the rejection is done according to the nearest-neighborhood approach. As the algorithm rejects an amount of data, the next iteration replaces them by a new random sample. Iterations of data rejections and replacements continue until the algorithm converges.

The decision inequality for activating the rejection is given by the following rule

$$\text{If } (N_{trn}-N_{max,TRN}) > 0, \text{ then rejection is taking place.} \tag{18}$$

The methodology continues by sorting the rows of the matrix $\mathbf{A} = [z\ \ddot{z}\ p_o\ \omega_o]$, from the smallest to the biggest, with respect to the selected array, which might be $\mathbf{p_o}$ or $\boldsymbol{\omega_o}$.

$$\mathbf{S}(s_p)=\text{sortrows}([\ \mathbf{z_r}\ \ddot{\mathbf{z}}\ \mathbf{p_o}\ \boldsymbol{\omega_o}],s_p) \quad , \tag{19}$$

where $\mathbf{A}=[\ \mathbf{z_r}\ \ddot{\mathbf{z}}\ \mathbf{p_o}\ \boldsymbol{\omega_o}]$ is the modified training dataset, and s_p is the binary parameter that takes the value of 1 for selected array $\mathbf{p_o}$ or the value 2 for selected array $\boldsymbol{\omega_o}$.

The approach for the data rejection from the array $\mathbf{p_o}$ or from the array $\boldsymbol{\omega_o}$ is fundamentally the same. For this reason, only the rejection with respect to the Euclidean distance between the elements in first array is demonstrated. Rejecting with respect to the array $\mathbf{p_o}$ characterizes the type I rejection process. Let $\mathbf{S_Q}=[\ p_{o,1};\ p_{o,2};\ldots\ p_{o,m-1};\ p_{o,m};\ p_{o,m+1}\ ;\ldots\ p_{o,n}]$ be an array, which includes sorted elements of the array $\mathbf{p_o}$. Formula (18) holds true for this array. An auxiliary array $\mathbf{S_{aux,Q}}$ is created by adding a new element at the beginning of array $\mathbf{S_Q}$, then by shifting down all rest elements, and finally by removing the last element $p_{o,n}$ from the array $\mathbf{S_Q}$,. The new element is equal to $p_{o,min}-(p_{o,max}-p_{o,min})/(N_{trn}-1)$. The auxiliary array takes the following format:

$$\mathbf{S_{aux,Q}}=\{\ p_{o,min}-(p_{o,max}-p_{o,min})/(N_{trn}-1);\ p_{o,1};\ p_{o,2};\ldots\ p_{o,m-1};\ p_{o,m};\ p_{o,m}\ ;\ldots\ p_{o,n-1}\ \} \tag{20}$$

Next, by subtracting the array $\mathbf{S_{aux}}$ from the array $\mathbf{S_Q}$, the array **D** is obtained, in which the h^{th} element of the array **D** represents the distance of the h^{th} element S_h of array $\mathbf{S_Q}$ from the adjacent smaller $(h\text{-}1)^{th}$ element S_{h-1}:

$$\mathbf{D=S_Q}\text{-}S_{\mathbf{aux,Q}} \tag{21}$$

The array **D** is added as a first column in the modified training dataset. The outcome is a matrix in the format $\mathbf{B} = [\mathbf{D\ z\ \ddot{z}\ p_o\ \omega_o}]$. Next, the rows of the matrix **B** are sorted based on the array that is indicated by parameter s_p. The sorting order is from the smallest element to the biggest one. Then, a number n_{si} is removed from the first rows in the sorted matrix. This number n_{si} equals the difference N_{trn}-$N_{max,TRN}$. Finally, by removing the first column from the sorted matrix, the outcome is the new reduced training dataset.

The above description refers to the type I rejection process. The method is adapted to the rejection type II or to the rejection type III, by considering the array $\boldsymbol{\omega_o}$ or both arrays $\mathbf{p_o}$ and $\boldsymbol{\omega_o}$, respectively. The prerequisite conditions for choosing each one of the three types of rejection are explained in the next subsection. The subject of the coming subsection is to present the flowchart of the MOJO procedure in a graph that brings all the parts together.

3.6.4. MOJO Procedure Flowchart. Figure 3.7 depicts the flowchart for the MOJO procedure. The following lines explain the consecutive steps that are undertaken in the flowchart.

The MOJO procedure starts by collecting data up to the initial number N_{min}, without any restriction. After the minimum dataset size is reached, the iterations continue, but a new check loop is repeated at each new data sampling. The check modules examine whether the datasets meet the desired convergence criteria or not. If the criteria are met, then the procedure ends, otherwise, the samplings continue.

However, sometimes the MOJO procedure reaches the maximum value $N_{max,trn,}$ without having acquired a dataset that meets the other two convergence criteria that concern the dispersion and learning quality. In this dead end situation, the rejection process offers a solution.

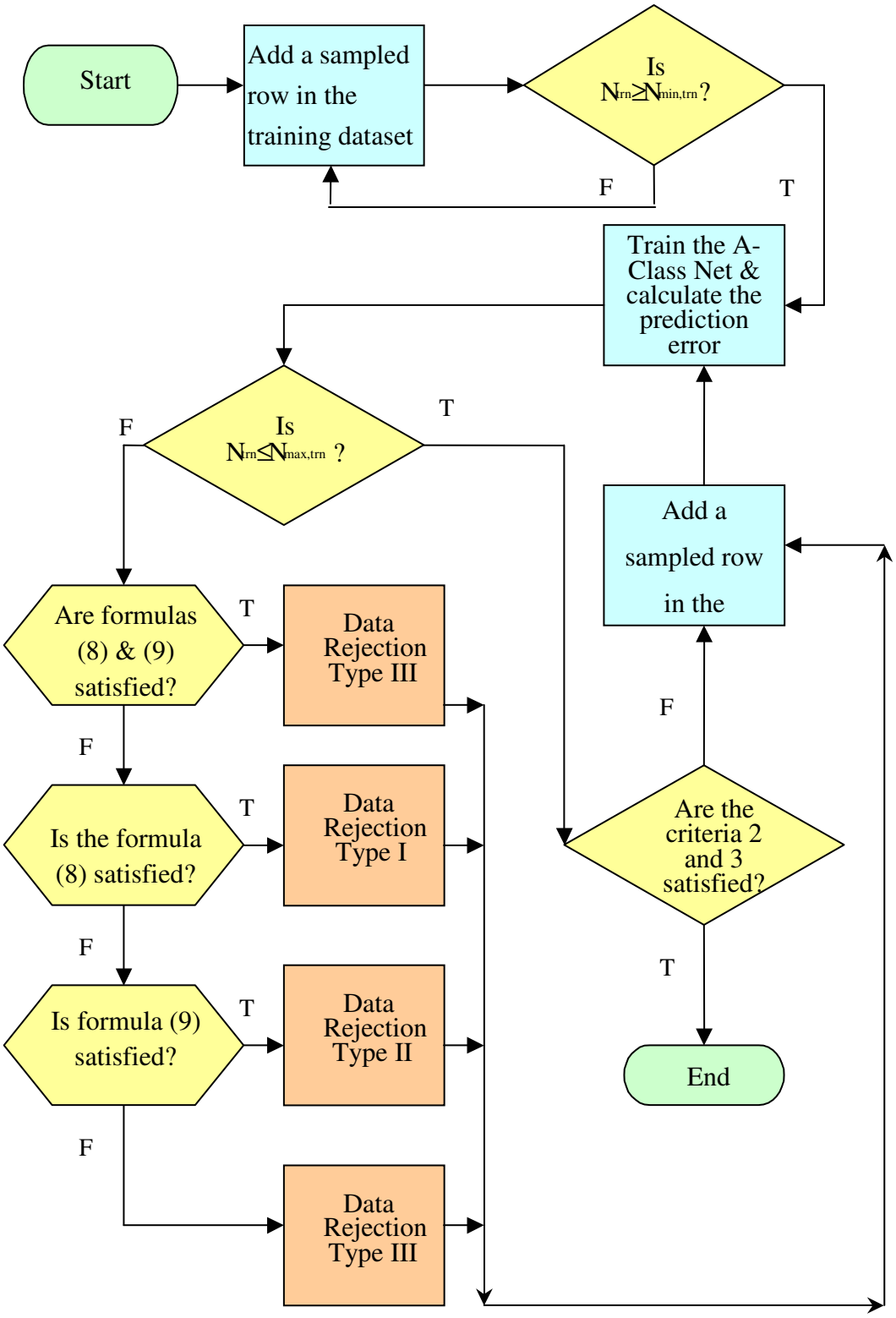

Figure 3.7. Flowchart for the MOJO procedure

In Figure 3.7, type I rejection will be activated, if formula (8) is satisfied, but formula (9) is not met. In other words, the type I rejection will start, if the data in the array po are not divided equally into a number of s equal ranges. In contrary, the type II rejection will be activated, if formula (8) is satisfied, but the formula (9) is not met. Finally, the type III rejection takes place in the following two cases. In the first case, the formulas (8) and (9) are met for both the po and ωo arrays, but the training dataset has exceeds the desired size limits. In the second case, the dispersion criteria are not met for either the load amplitude or for the load frequency arrays. In the Figure 3.7, the letter T denotes the truth value and the letter F denotes the false value.

The coming subsection introduces a procedure that collects a testing dataset for the Damage Diagnostic Decision. This procedure has several common points with the MOJO approach.

3.7. CREATING THE DIAGNOSTIC DECISION DATASET

This subsection introduces a procedure for building up the Damage Diagnosis Decision Dataset, which is written as 3D dataset or as 4D, in short. The aforementioned dataset is a subset of the dataset that is used for the testing of ANFIS. Building up the 4D is a procedure similar to the MOJO procedure, which was introduced in Subsection 3.6. This procedure iterates data sampling cycles until the two convergence criteria are met. The first criterion concerns the datasets size, while the second criterion concerns the data diversity. In addition, the procedure includes a rejection process, which is engaged in order to keep the 4D within the desired size. The mathematical formulation for the convergence criteria is given below.

In the first criterion, the size of the decision dataset is defined to be bigger that the selected minimum size of the testing dataset $N_{min,tst}$ and for practical reasons it should be smaller than the size of the training dataset.

$$N_{mim,4D} \leq N_{4D} \leq N_{max,tst} = N_{trn} \quad , \qquad (22)$$

where $N_{min,4D}$ is the bottom value for the size of Damage Diagnostic Decision Dataset, N_{4D} is the size of Damage Diagnostic Decision Dataset, $N_{max,tst}$ is the maximum size of the testing dataset, N_{trn} is the size of the training dataset.

The criteria for selecting the minimum value $N_{min,4D}$ are similar to those described in Subsection 3.6.2 for selecting the minimum size of the training dataset.

In order to satisfy the testing dataset diversity criterion, data are collected until the following inequalities are satisfied:

$$(p_{o,min}+p_{o,max})*(1-\varepsilon)\leq 2*\text{median}(\mathbf{p_{o,4D}}) \leq (p_{o,min}+p_{o,max})*(1+\varepsilon) \quad , \quad (23)$$

$$(\omega_{o,min}+\omega_{o,max})*(1-\varepsilon)\leq 2*\text{median}(\boldsymbol{\omega}_{\mathbf{o,4D}}) \leq (\omega_{o,min}+\omega_{o,max})*(1+\varepsilon) \quad , \quad (24)$$

$$p_{o,min}+\text{range}([p_{o,min},p_{o,max}])*(1-\varepsilon)\leq \min(\mathbf{p_{o,4D}})+2*\text{IQR}(\mathbf{p_{o,4D}}) \quad , \quad (25)$$

$$\min(\mathbf{p_{o,4D}})+2*\text{IQR}(\mathbf{p_{o,4D}})\leq p_{o,min}+\text{range}([p_{o,min},p_{o,max}])*(1+\varepsilon)) \quad , \quad (26)$$

$$\omega_{o,min}+\text{range}([\omega_{o,min},\omega_{o,max}])*(1-\varepsilon)\leq \min(\boldsymbol{\omega}_{\mathbf{o,4D}})+2*\text{IQR}(\boldsymbol{\omega}_{\mathbf{o,4D}}) \quad , \quad (27)$$

$$(\boldsymbol{\omega}_{\mathbf{o,4D}})+2*\text{IQR}(\boldsymbol{\omega}_{\mathbf{o,4D}})\leq \omega_{o,min}+\text{range}([\omega_{o,min},\omega_{o,max}])*(1+\varepsilon) \quad , \quad (28)$$

where $\mathbf{p_{o,3D}}$ is the load amplitude array of the Damage Diagnostic Decision (3D) dataset, $\boldsymbol{\omega}_{\mathbf{o,4D}}$ is the load frequency array of the 3D dataset, median is a MatLab function that calculates the median value of an array, IQR is a MatLab function that returns the interquartile range of an array, and ε is the tolerance. The interquantile range is defined as the difference between the third and the first quartile. Finally, on the above formulas the nomenclature terms range($[p_{o,min}, p_{o,max}]$) and range($[\omega_{o,min}, \omega_{o,max}]$) are the service ranges of the potential load amplitude values, and of the potential load frequency values, respectively.

The above six formulas aim to guarantee the data dispersion for the 3D dataset. The scope is that the decision dataset has similar statistical characteristics as the training dataset. Formulas (23) and (24) harmonize the measures of the central tendency between the two datasets. The formulas (25) to (28) enforce that half of the decision data occupy a range that equals the half of the relevant service range. By imposing these diversity restrictions, it is avoided to obtain a decision dataset that is concentrated in a very narrow interval of the service space. The above criteria are weak diversity conditions compared to the diversity criteria imposed to the training dataset by formulas (8) and (9). Those

training diversity conditions required that the training dataset included representative values all along the service ranges. It would be unpractical and unnecessary to apply those strict dispersion conditions in the case of the 3D dataset.

This paragraph closes the third section, which concerned with the modeling of the Damage Diagnostic Algorithm. The coming section will explain this model architecture through a numerical application.

4. NUMERICAL APPLICATION

4.1. INTRODUCTION

Section 3 was devoted to the detailed modeling of the Bridge Damage Diagnostic System. This section shows how the ideas of the previous section work in practice. A numerical example sheds light into the abstract models of the Damage Diagnostic System.

The material in Section 4 is organized in three subsections. Subsection 4.2 begins by introducing the simulation experiment. Then, Subsection 4.3 provides information about the generation of the training dataset. The closing Subsection 4.4 presents the simulations for generating the testing dataset.

4.2. INTRODUCING SIMULATION

The numerical application, which is the topic of this section, is evaluated through Monte Carlo Simulations. This subsection introduces the simulation experiment, by listing the consecutive experiment phases and the simulation characteristics.

All formulas and procedures for the simulation experiment are embedded in a MatLab coded program. The simulation is based on random processes. So each time the algorithm runs, it comes up with different results. However, this does not impose a problem, because the function and the evaluation of the Damage Diagnostic System is performed by estimating mean values from several convergent randomly simulations. This is a standard evaluation through the Monte Carlo Simulation methodology.

The simulation experiment is executed in six consecutive phases, namely the training datasets compilation through the MOJO procedure, the Neuro-Fuzzy Systems training, the testing datasets compilation through the 4D procedure, the Neuro-Fuzzy Systems testing, and finally the statistical calculation of the damage rate.

The next of the section is devoted to the detailed presentation of the simulation phases that concern the training datasets compilation.

4.3. TRAINING DATASET GENERATION

The MOJO procedure, which was introduced in Subsection 3.6, is an iterative process for sampling the training data. This subsection provides a numerical simulation for the MOJO procedure.

The training data for the A-Class ANFIS consist of two input arrays and one target output arrays. The target array includes values of the excitation loads that are sampled from various statistical distributions. Once the excitation loads are known, the bridge response parameters z and $\ddot{\mathbf{z}}$ are calculated, through the equation of motion of bridge model, which is presented in D. Danilatos (2008).

The selected bound values for MOJO procedure in our simulation experiment are summarized in Table 4.1. The convergence criteria formulas and their relevant nomenclature have been introduced in Subsection 3.6.2. In this table, it can be seen that the parameter N_s takes the value one, so each segment should include at least one element. Concerning the dataset dispersion, the service range is divided into s=10.

Figure 4.1 presents an example of a simulated multidimensional training dataset for the A-Class Network. This set is the outcome of the MOJO procedure. From the other part, the training dataset of the B-Class Neuro-Fuzzy Networks is a 160-by-3 dataset.

A segment of the B-Class training dataset is given in Table 4.2. Each row represents a different vehicle event. The two first columns include the two inputs to the B-Class N/F Network, while the target output is located in the third column.

Figure 4.2 compares the time-histories for the inputs and the target output for the B-Class Adaptive Neuro-Fuzzy System.

4.4. TESTING DATASET GENERATION

The previous subsections dealt with the training datasets, while this one provides an example for the testing datasets.

The testing and the training datasets have similar format, size and quantity. Also, there exist testing datasets for the two classes of networks; similarly as it was the case

Table 4.1. Bound values for MOJO procedure convergence criteria

1) Size Criterion	
$N_{min,trn}$	40
$N_{max,trn}$	160
2) Dataset dispersion criterion	
P_{min}	$5.426*10^{-6}$
P_{max}	0.2722
$\omega_{o,min}$	0.0056
$\omega_{o,max}$	0.5556
s	10
N_s	1
3) ANFIS learning quality criterion	
$e_{lim,chk}$	0.0012
$\sigma_{lim,chk}$	0.0019
$e_{lim,trn}$	$1.20*e_{lim,chk}=0.0014$
$\sigma_{lim,trn}$	$1.10*\sigma_{lim,chk}=0.0021$

with the training datasets. However, there are two main differences between the testing and training datasets.

The first difference between the two kinds of datasets concerns the bridge damage state. In the case of the training data, the bridge is undamaged. In contrast, the testing set includes data from the same bridge with various degrees of damage. The second difference is that the two datasets are the outcome of two different iterative sampling procedures. The MOJO procedure is used for the training datasets, and the 4D procedure is for conducting testing datasets sampling.

Therefore, two kinds of simulations are required in order to generate the testing data. The first simulation concerns the damage state development through time. For different testing subsets, the damage rates take values between 0 and 8 percent. The

latter simulation concerns the generation of random testing data and their sampling through the 4D procedure. A numerical example about this simulation is given below.

Once the raw testing data are generated through random numbers simulations, the 4D procedure is applied in order to screen the data that are compiled for the damage diagnostic decision (3D) subsets. As it was set down in Subsection 3.7, this procedure samples data triplets so the constructed 3D dataset complies with two convergence criteria.

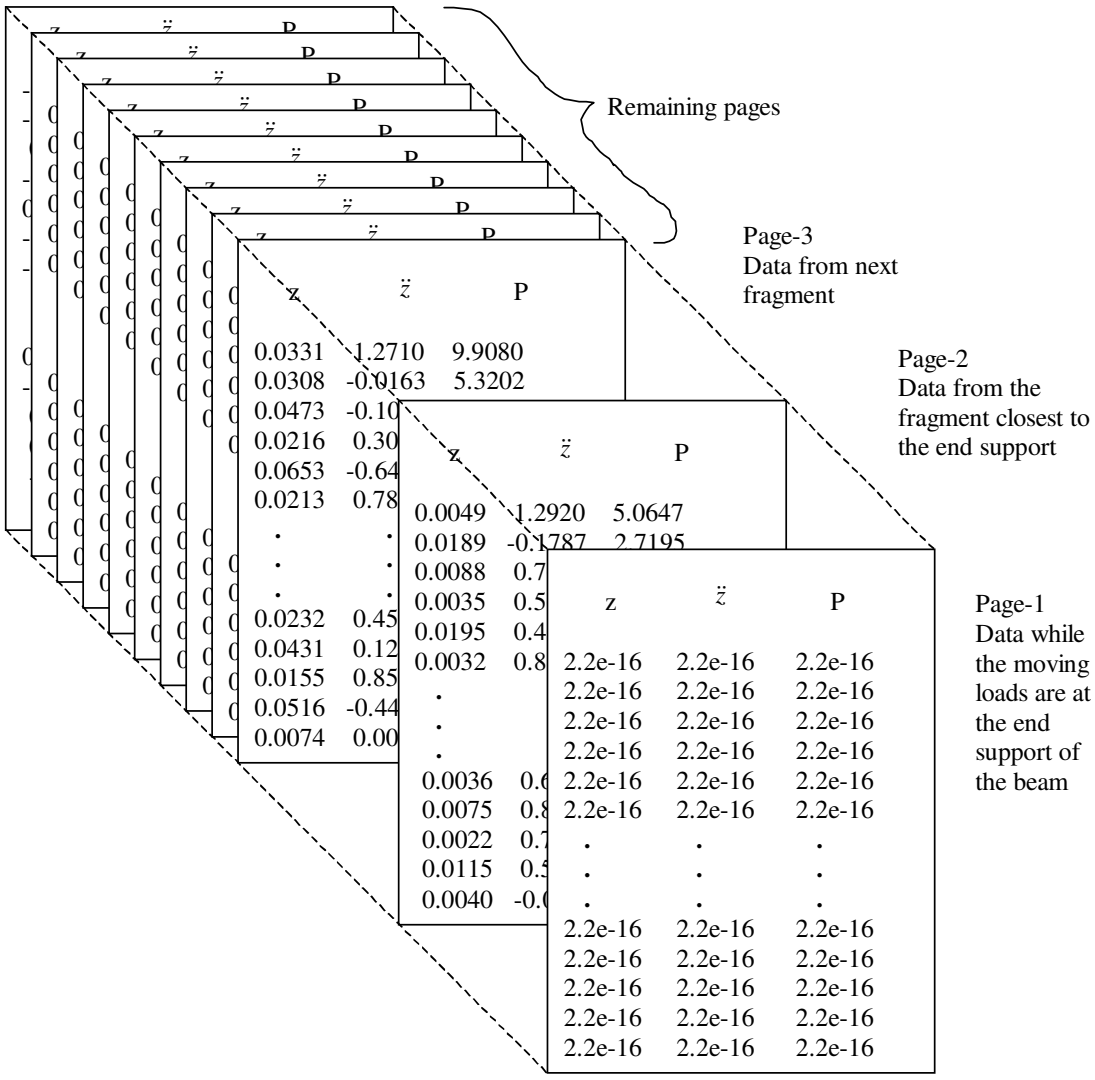

Figure 4.1. Training datasets for the A-Class learning network

Table 4.2. Training dataset for B-Class Neuro-Fuzzy Networks

p_o	ω_o	RMS error
0.0081	0.0341	0.0014
0.0556	0.0589	0.0004
0.0359	0.1972	0.0008
0.0380	0.4941	0.0007
0.0445	0.3669	0.0001
0.0047	0.1106	0.0010
.	.	.
.	.	.
0.1677	0.3229	0.0000
0.0762	0.1906	0.0000
0.2300	0.1301	0.0000
0.1047	0.4800	0.0002
0.0283	0.1323	0.0006

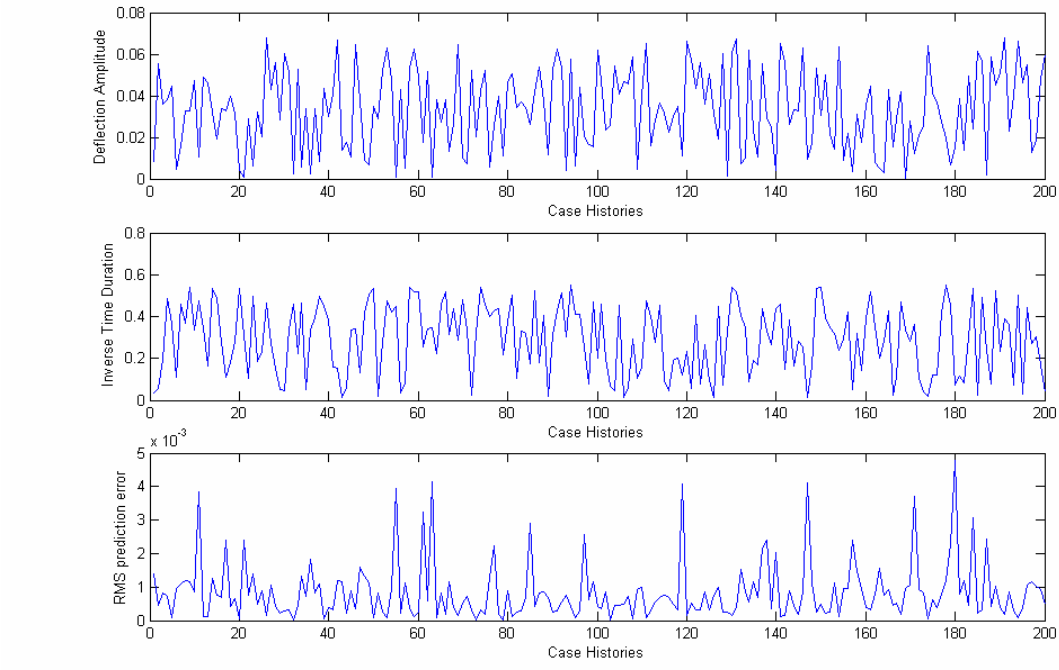

Figure 4.2. Training inputs and target output for the B-Class ANFIS

For this simulation example, the choice is that the 3D dataset includes at least 40 elements and it contains fewer than 160 elements. The size criterion inequalities from the formula (22) are written as follows:

$$N_{mim,4D}=40\leq N_{4D}\leq N_{max,tst}= N_{trn} =160 \quad ,$$

Concerning the dataset diversity criterion, the bounds values for training data, which are included in Table 4.1 and the dataset diversity inequalities (23) and (28), are adopted accordingly.

The outcomes of the simulation phases, which were presented in the sections 4.3 and 4.4, are the training dataset TRN1 and the testing dataset TST1. The Monte Carlo simulation provides several data realizations. For this reason, apart from first series of datasets, the Monte Carlo simulation generates 19 different triplets of datasets TRN2, CHK2, TST2, and TRN20, CHK20, TST20.

The coming section presents the findings concerning the damage diagnosis, and evaluates the systems performance.

5. FINDINGS

5.1. INTRODUCTION

The previous section introduced to the simulation experiment that is used in this thesis in order to investigate the proposed Damage Diagnostic System. So far, the simulation that generated the training and the testing datasets is presented. This section makes available the research results. The material in this section is organized into two subsections, as follows. The first subsection studies the convergence of the data sampling procedures. Then, the second subsection presents the damage diagnosis results and the evaluation of the performance of the developed model.

5.2. CONVERGENCE STUDY

This subsection studies the convergence of the two developed sampling procedures. In particular, Subsection 5.2.1 deal with the MOJO procedure, which concerns training data, while Subsection 5.2.2 investigates the 4D procedure, which concerns the testing data.

5.2.1. Convergence for the MOJO Procedure. The training dataset for this simulation experiment is not derived as the result of a single iteration, but rather it is the outcome of several cycles of data samplings and data rejections, which were based on the MOJO procedure. The modeling for this procedure was presented in Subsection 3.6, while the bound values for convergence were selected in Subsection 4.3. This subsection validates the developed MOJO procedure by studying how it converges at the desired training dataset, after satisfying the three convergence criteria. Each convergence criterion is presented in a separate subsection.

5.2.1.1 Training dataset size criterion. The first convergence criterion for the MOJO procedure concerns the training dataset size. Figure 5.1 plots the convergence of the training dataset size, as a function of the accumulate number of sampled data. During the data sampling, note at this figure that the training dataset size increased linearly and unrestricted from zero up to the maximum bound value $N_{max} = 160$. After having reached

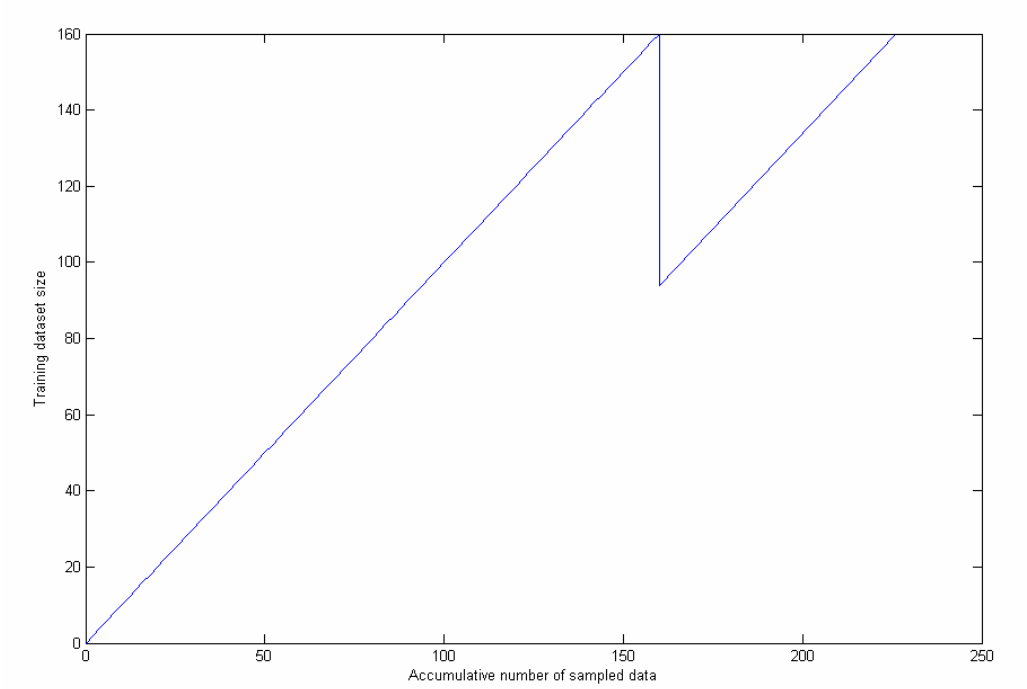

Figure 5.1. Convergence for MOJO procedure with respect to the training dataset size

the maximum bound value N_{max}, the rejection process was activated. In the simulation that is depicted in Figure 5.1, the rejection process removed 66 elements, so the training dataset dropped to the size of 94 elements. The tooth in the saw-like curve shows the data reduction, during the rejection process. The data rejection kept the dataset size within the desired maximum value of 160 elements. The rejected data were replaced by freshly sampled ones. The MOJO procedure finished, when all convergence criteria have been satisfied.

5.2.1.2 Training data dispersion criterion. The second criterion for the MOJO process is related with the training data dispersion. Recall from the Subsection 3.6.2 that the training dataset dispersion is secured by spreading out the two harmonic parameters of the excitation load, namely the amplitude and the frequency. At the Subsection 4.3, the potential ranges for each of the two harmonic parameters were divided into s=10 equal sub-ranges. To satisfy the dispersion criteria, it was required that all the sub-ranges contained one element at least.

The following five figures, illustrate a convergence example of the MOJO procedure with respect to the data dispersion criterion. At first, Figure 5.2 shows the time development for the dispersion of the two considered parameters. In this figure, the Y-axis parameter is the number of sub-ranges that contain one element at least. The blue solid line depicts the dispersion with respect to the load amplitude p_o, while the green dotted line represents the dispersion of the load frequency parameter. In the simulation experiment, the dispersion measures were increasing, during the sampling of the initial 160 data. However, when the initial 160 elements had been collected, only the amplitude dispersion was met, but the frequency dispersion goal had not yet reached. After this point, cycles of data rejections and samplings facilitated the MOJO procedure to convergence.

The data dispersions with respect to the two parameters are better illustrated in the following four histograms, from Figure 5.3 to Figure 5.6. From the one hand, histograms Figure 5.3 and Figure 5.4 depict the dispersion for the population of the 160

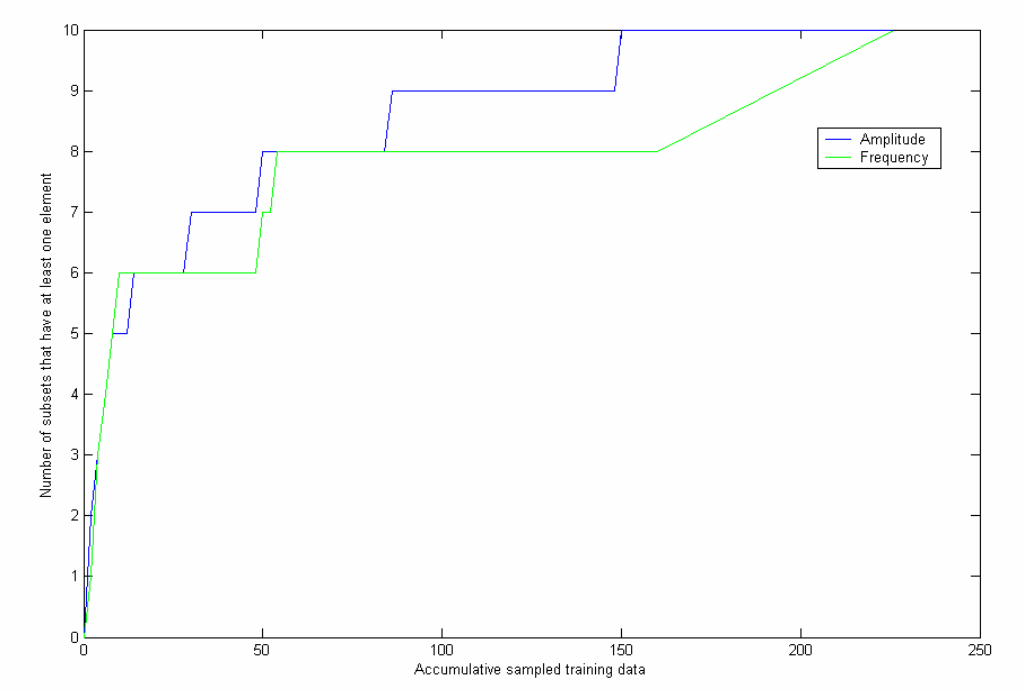

Figure 5.2. Data dispersion criteria versus time

initially sampled data, and from the other hand, Figure 5.5 and Figure 5.6 present the corresponding histograms for the convergent training dataset. Note that the final training datasets, which were the result of continuous rejection-samplings cycles, contained 160 data elements, as well. Figure 5.3 and Figure 5.5 concern the excitation amplitude variable, while Figure 5.4 and Figure 5.6 deal with excitation frequency parameter.

The following observations are made on these four figures. First, as it should be expected all the histograms exhibit normal distributions. Second, the potential ranges of the x-parameters are divided into ten sub-ranges by vertical red lines. In Figure 5.3 and Figure 5.4, observe that some of the extreme left bound sub-ranges contain no data elements; this means that the dispersion criteria are not met yet. By contrast, compare the previous two figures with Figure 5.5 and Figure 5.6, to find out that the convergent dataset is spread out in a wider area and all ten sub-ranges contain one element at least. In overall, the dispersion criterion reduces the theoretically infinite number of the training

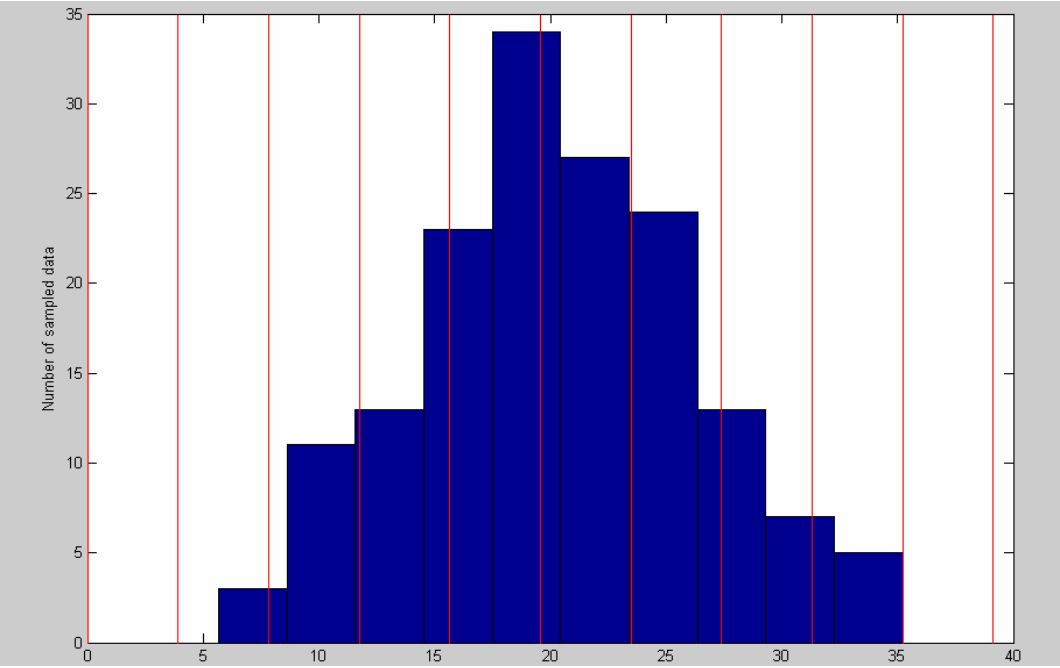

Figure 5.3. Histogram of the load amplitude for the 160 initially sampled data elements

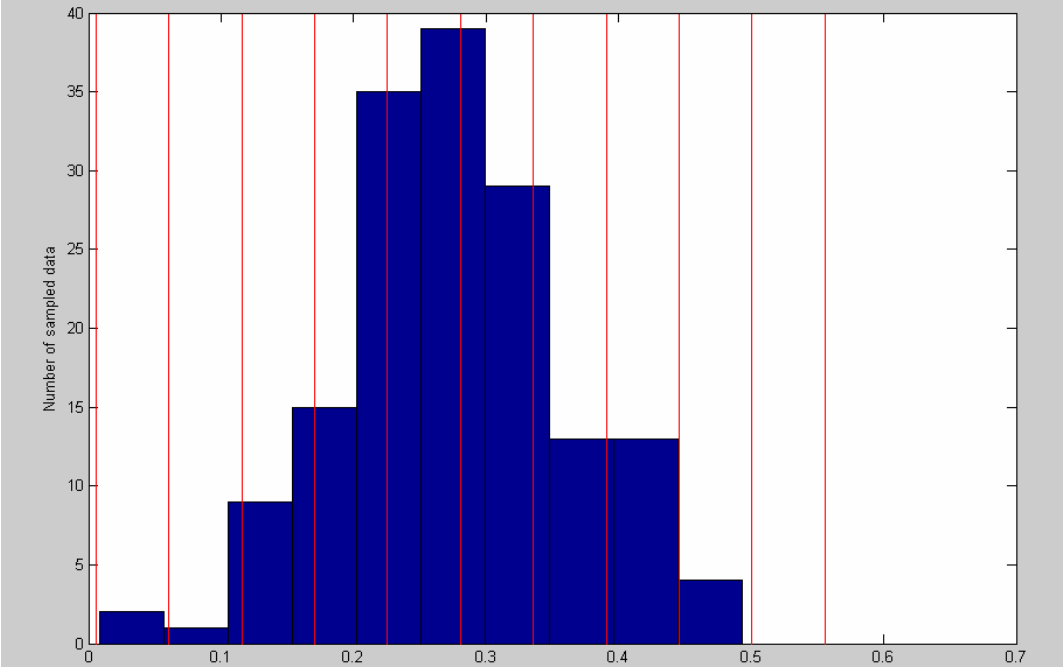

Figure 5.4. Histogram of the load frequency for the 160 initially sampled data elements

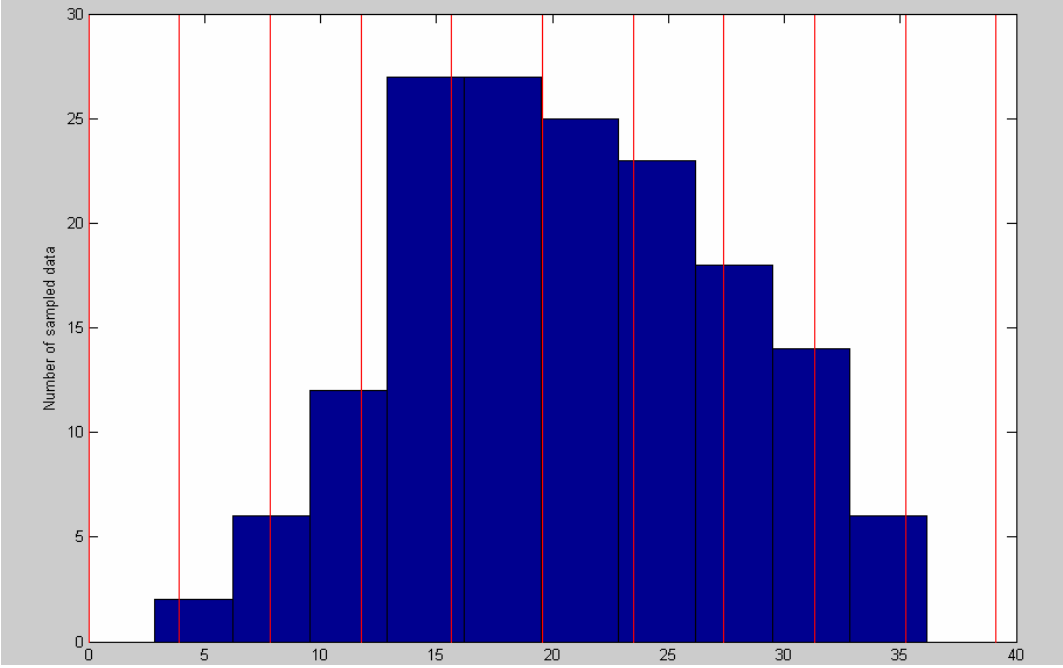

Figure 5.5. Histogram of the load amplitude for the final convergent dataset

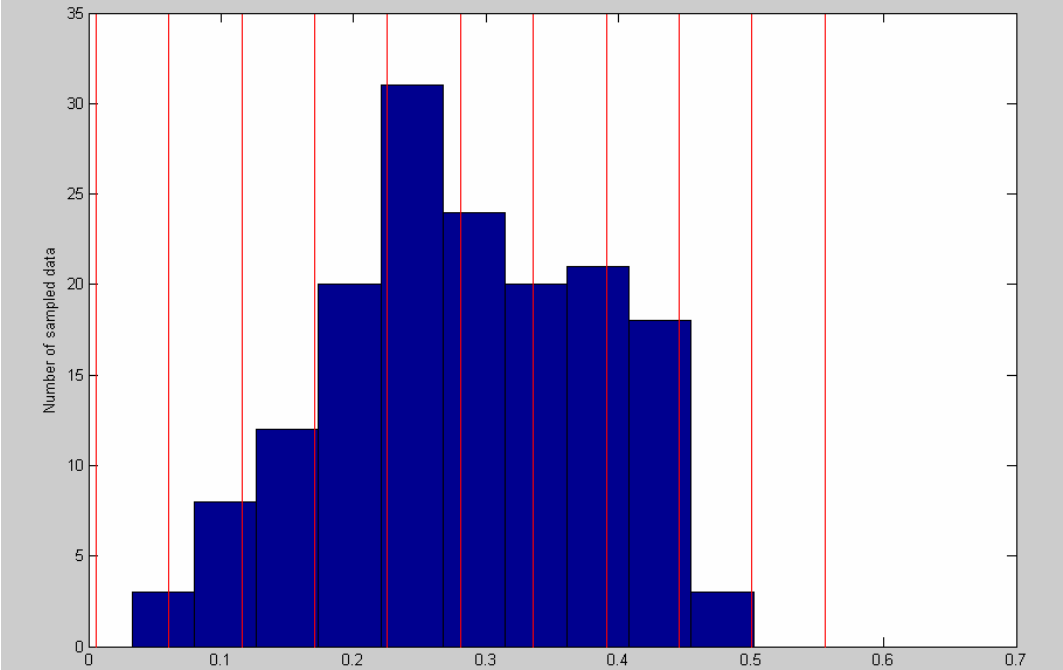

Figure 5.6. Histogram of the load frequency for the final convergent dataset

data that might be potentially sampled into a few values that contain most of the relevant information.

5.2.1.3 Performance criteria. The third category of the convergence criteria for the MOJO procedure concerns the learning quality of the A-Class Neuro-Fuzzy Networks. These criteria establish preliminary performance indices for the Diagnostic Algorithm. The learning quality criteria observe two statistical parameters of the RMS prediction error of the ANFIS, namely the arithmetic mean and the standard deviation. The following two figures depict the development of these two statistical parameters, as the training datasets vary through time. Figure 5.7 shows how the mean prediction error develops during the training dataset samplings. From the other part, Figure 5.8 depicts the time development for the standard deviation of the prediction error. Both figures have the same characteristics. The horizontal red poly-line denotes the desired upper bound. The blue poly-line denotes the statistical parameter that is obtained by different training datasets during MOJO procedure. From the other part, the green poly-line

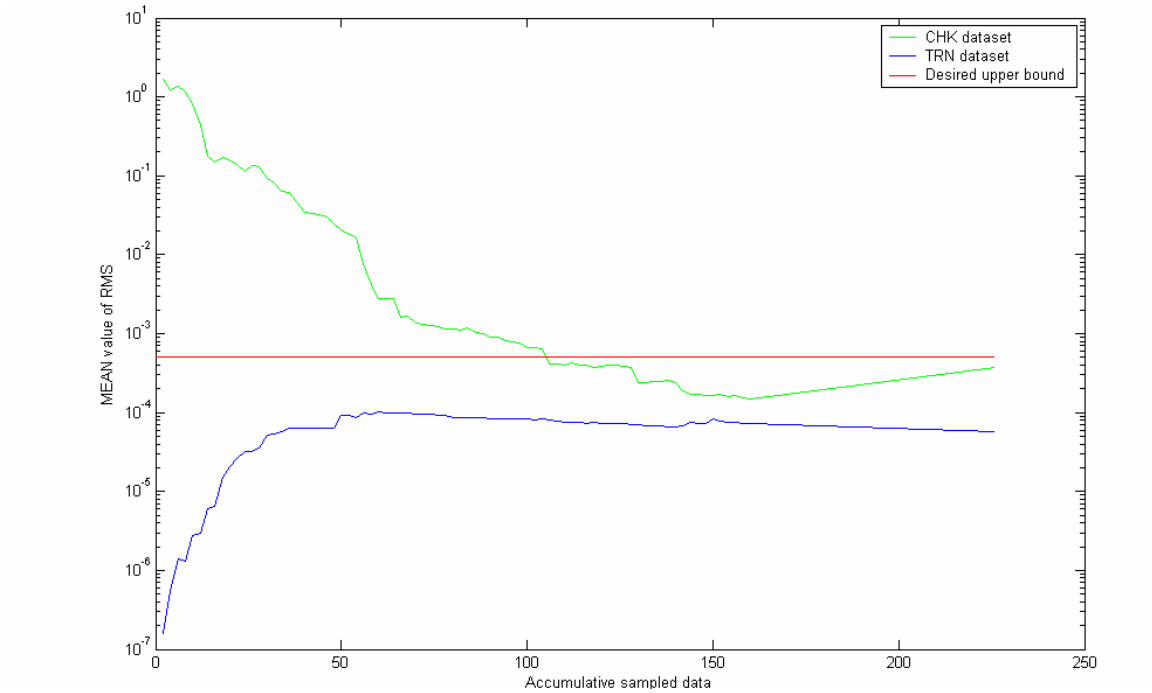

Figure 5.7. Convergence study for the average prediction error

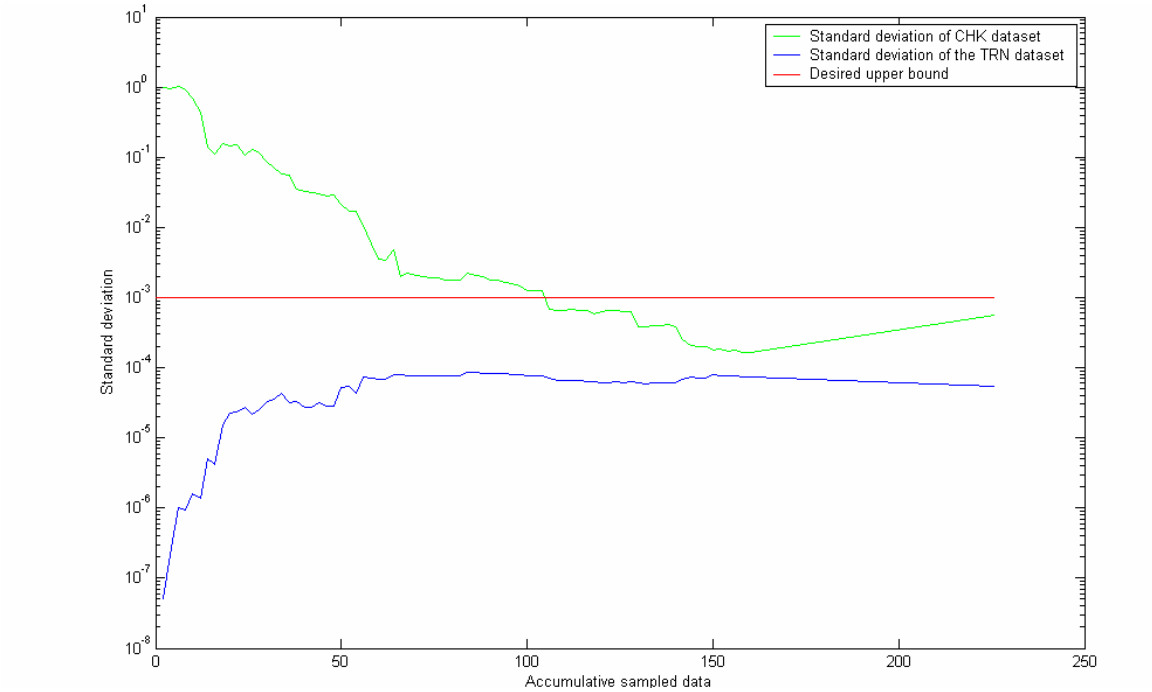

Figure 5.8. Convergence study for the standard deviation of the prediction error

represents the statistical parameter of the corresponding checking datasets. The x-axis has linear scale, while the y-axis scale increases logarithmically.

In Figure 5.7 and Figure 5.8 observe that the prediction errors for the training datasets (blue lines) were lower than the desired upper bound. In the initial phase of the MOJO procedure, when the training dataset contained approximately less than fifty samples, the prediction for the training data was very successful, while the prediction error for the checking dataset was very high. This situation, which is called overtraining, happened because the learning system was trained with datasets that were not adequately diverse and large. As the MOJO procedure moved ahead, the networks generalization improved, due the fact that the training dataset was larger and it included more diverse elements. In Figure 5.7 and Figure 5.8, observe that the prediction errors for the training and for the checking datasets were tending to equalize, as the accumulative sampled data reached the size of 160 elements. After this point, the MOJO procedure started to reject a part of the training data, in order to replace them with newly sampled ones. This replacement causes a distortion on the distribution of the training dataset compared to the initial distribution from which both the checking dataset and the raw training data had been sampled. Due to these different distributions, the prediction error for the checking datasets increased slightly, but nevertheless it remained below the desired goal value.

Figure 5.1,Figure 5.2, Figure 5.7, and Figure 5.8 are directly comparable, because their x-axis and scale are the same. These plots depict the time development for the two different convergence criteria. By comparing these four plots, it is found that the convergence criteria were reached at the following sequence. The two performance criteria were met, after the first 106 initial elements had been sampled. The data sampling continued until the dataset assembled 160 elements, which was the ceiling value for the size criterion. Because at this moment, the dispersion criterion was not met yet, the reduction process had been initiated. This process removed a number of 66 elements from the dataset. Then, by sampling 66 additional data, the convergent training dataset satisfied the dispersion criteria. The reduction-sampling cycles increased the datasets diversity.

In Figure 5.7 and in Figure 5.8, the smaller the training dataset was, the better the prediction accuracy for the training data was. This was due to the ANFIS overtraining

and as a result the network was not capable to predict previously unseen checking data. When the training dataset had attained the crucial bulk of about 100 elements, then the ANFIS was capable to predict the random checking data with an acceptable accuracy. The prediction accuracy for the training data remained almost unchanged, after the dataset had attained the moderate size of about 60 elements. The curves for the checking data in Figure 5.7 and Figure 5.8 show that the ANFIS predictability was improving until the initial 160 elements had been collected. After this point, there the prediction error for the checking datasets increased slightly.

5.2.2. Convergence study for the testing dataset. The procedure for generating a Diagnostic Decision Dataset, which was coined as the 4D procedure, was introduced in Subsection 3.7. This section illustrates the convergence of a random Diagnostic Decision Dataset.

The 4D procedure is an iterative process that stops when the two convergence criteria are met. These criteria concern with the dataset size and with the dataset dispersion. Figure 5.9 and Figure 5.10 depict the time variation of these parameters the dispersion of which was defined in the formulas from (23) to (28). It is observed that the interquantile ranges of the two observed parameters fall within desired bounds. The two horizontal red lines define the desired bounds for the dispersion criteria. The green poly-line demonstrates the change of the dispersion indices, as the dataset size increases. This poly-line swings between the bound limits horizontal lines. In addition, note that the convergent dataset contains 26 elements, so its size is within the desired bounds. The fast convergence of the sampling procedure is an advantage because it guarantees the early damage detection.

Figure 5.11 combines information from the Figure 5.9 and from the Figure 5.10. The poly-line relates the interquantile range of the amplitude to the interquantile range of the frequency. The beginning of this poly-line is marked with a small circle, while the end of this poly-line is marked with a little triangle. The sides of the yellow quadrangle define the goal bounds for the dispersion criteria. The beginning of this poly-line, which is marked with a small circle, represents the 20th event, while the end indicates the 26th event.

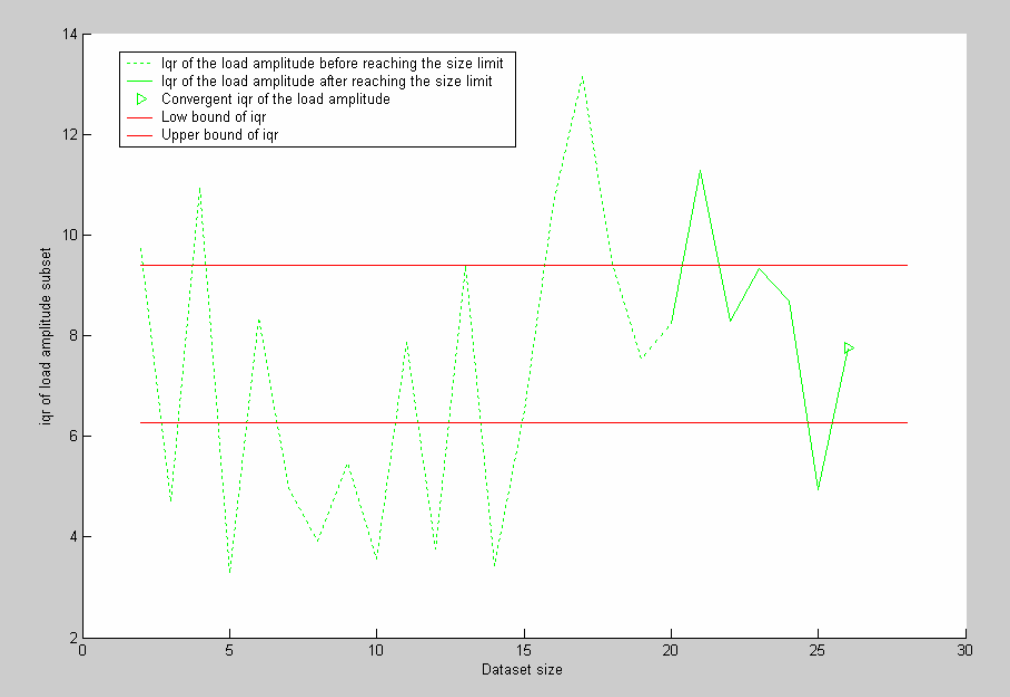

Figure 5.9. Convergence study for the first dispersion criterion

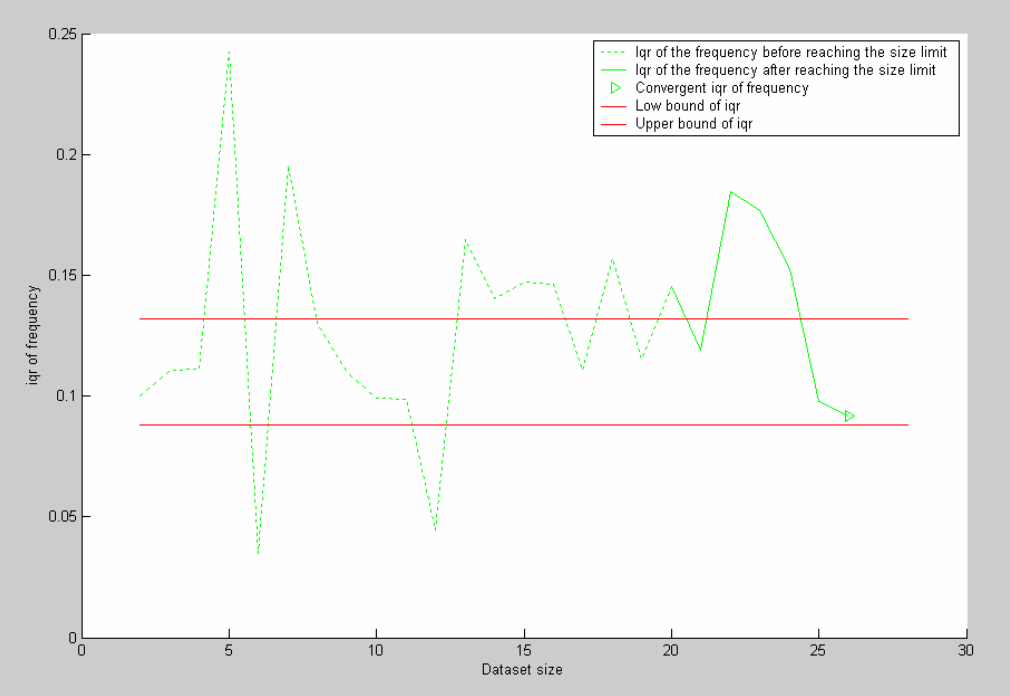

Figure 5.10. Convergence study for the second dispersion criterion

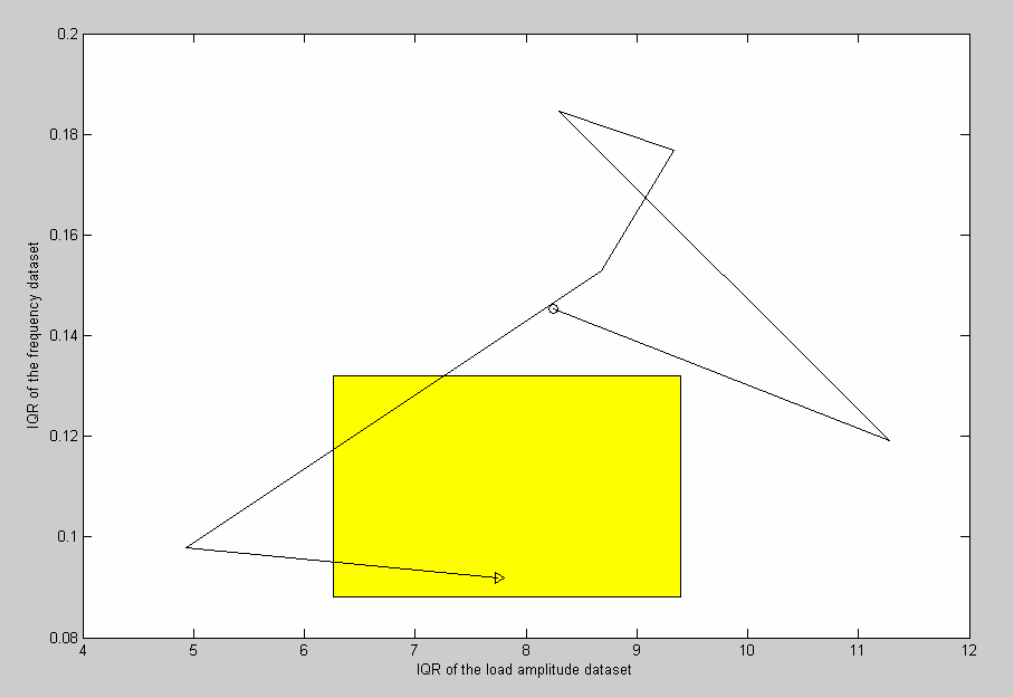

Figure 5.11. Relating the two dispersion indices

5.3. DAMAGE DIAGNOSIS

This subsection presents the results taken from the Damage Diagnostic Algorithm. As it was explained in Subsection 3.7, the algorithm makes diagnostic decisions that are based, not on a single vehicle event, but on a diagnostic decision subset. In Figure 5.12, the red fluctuating line shows the predicted mean damage rates for such a random diagnostic decision dataset. This fluctuation is a statistical phenomenon, which is typical in any Monte Carlo simulation. It is assumed that during all these simulated vehicle events, the real damage rate remained constant at 7%, which is demonstrated by the blue horizontal line, in Figure 5.12. By averaging all the predicted damage rates, the prediction for the damage rate has the absolute value 6.9%.

The next Figure 5.13 depicts the average diagnostic results for different decision subsets. However, because the difference between the predicted and the expected damage rates would be hardly distinguished, the damage rates are substituted by the Diagnostic Systems prediction error, which is calculated as the difference between the

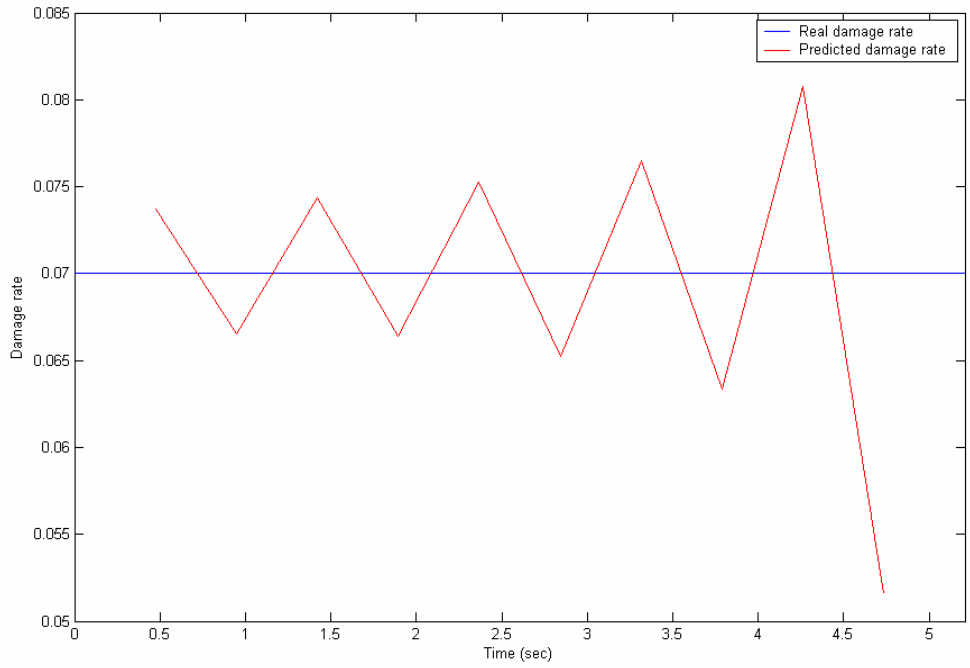

Figure 5.12. Real and predicted damage rates for a vehicle event

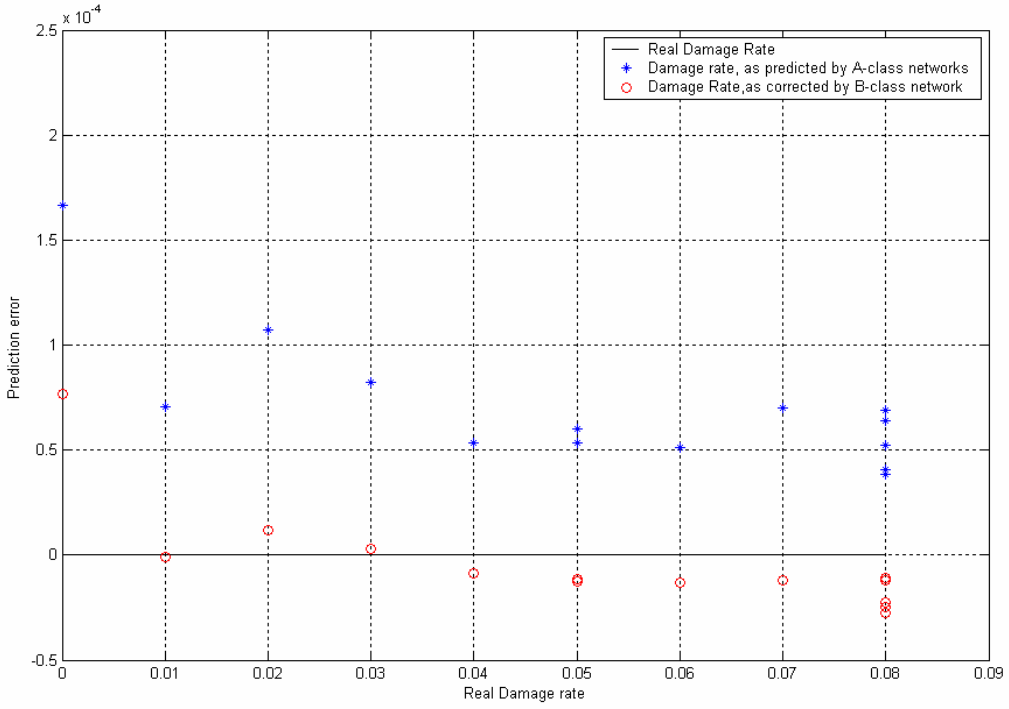

Figure 5.13. Absolute prediction errors

estimated and the expected damage rates. In this way, a graphical representation on a finer scale is taken.

The absolute prediction errors are plotted as red circles marks in Figure 5.13. In the same figure, the blue star marks represent the initial estimation that is based on the A-Class Network only, before applying any correction by using the B-Class Network. In Figure 5.13, the solid horizontal line represents the ideal prediction rate, which has the value zero.

This figure shows that the prediction error for the final damage rate was reduced considerably, compared to the initial damage rate. However, in certain instances, this final prediction error took negative values, which implied that the corrective subtrahend quantity was more than it was required. Using estimation results that include negative prediction error might lead to situations in which the structural damage goes undetected or underestimated. From the other part, as shown in Figure 5.13, the prediction errors for the initial damage rates were quite low and practically negligible. Therefore, it is

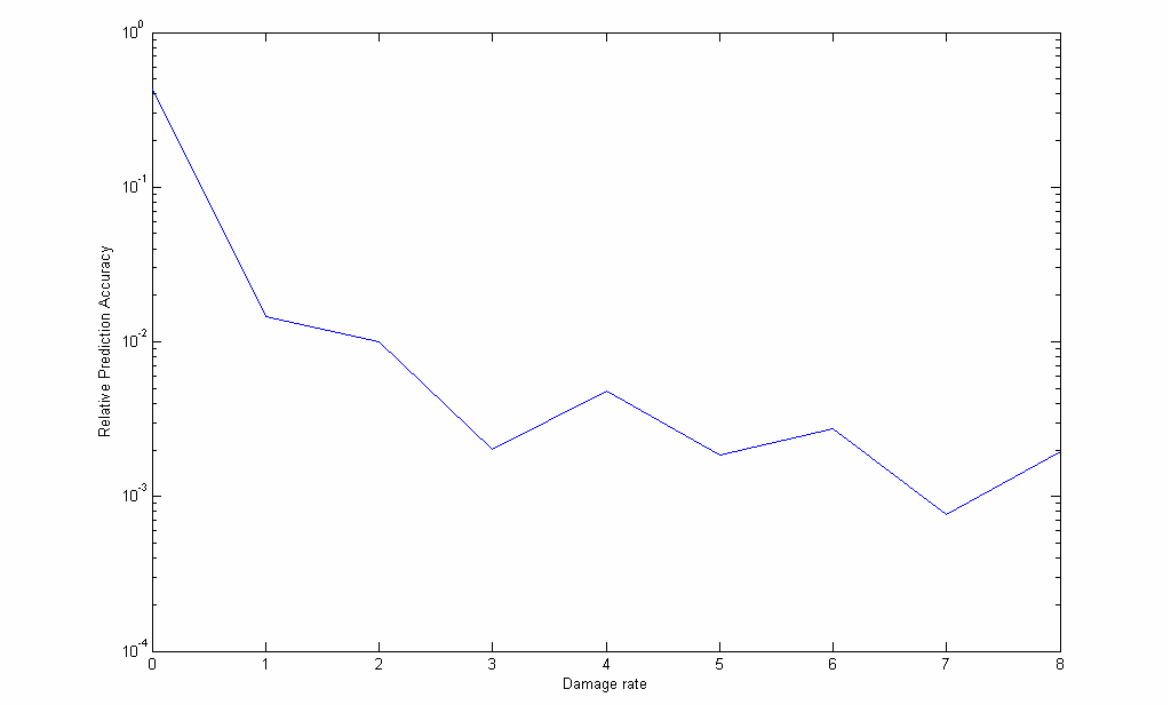

Figure 5.14. The relative prediction error versus the actual damage rate

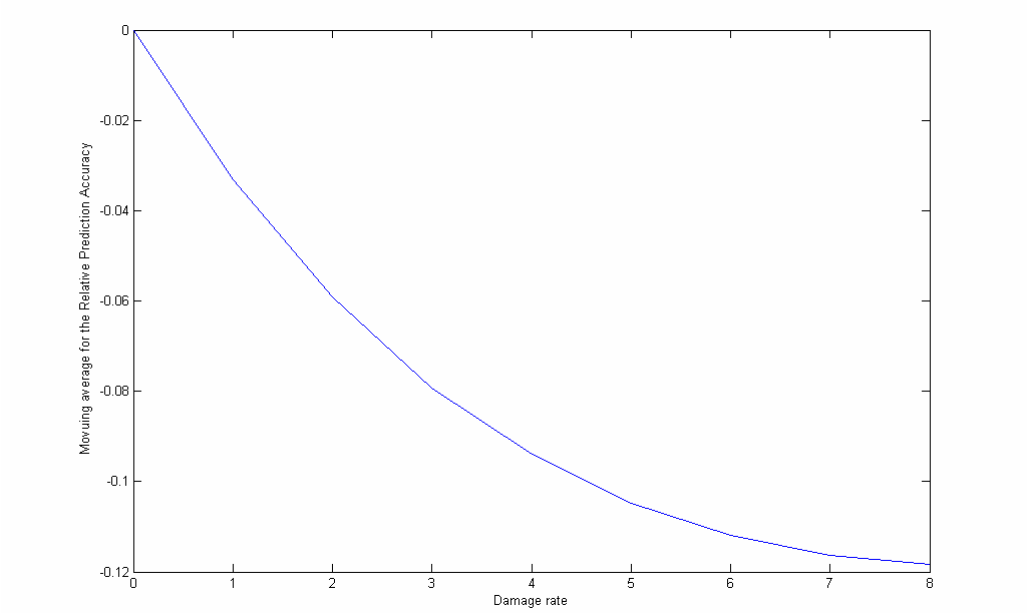

Figure 5.15. Moving average for the relative prediction accuracy versus the actual damage rate

preferable to consider the initial damage rate rather than use the B-Class Network corrective action.

From the other hand, Figure 5.14 plots the relative prediction accuracy versus the damage rate. Theoretically, the relative prediction rate of the undamaged structure should be indefinitely high. However in this figure, the relative prediction error took a high value that has indicative significance. The y-axis in this figure is logarithmic. Finally, in Figure 5.15, by plotting the Moving Average Convergence/Divergence function for the relative prediction accuracy, it is remarked that as the damage rate increased, the relative prediction error decreased, in an exponential decrease rate. Therefore, the diagnosis of the higher damage rates in more successful, when it is compared with the diagnosis of the lower damage rates.

This section presented the outcomes that were obtained through simulations of the Damage Diagnostic System. The coming section will further discuss these findings.

6. DISCUSSION –CONCLUSIONS

6.1. INTRODUCTION

This thesis attempted to design a Damage Diagnostic Method for structural bridges. The automatic on-line system identifies and quantifies damage by extracting information from vibration signals, during dynamic incidents.

This last section summarizes the research findings and the conclusions. The material is organized in three parts. The first part, which extends from Subsection 6.2 to 6.5, discusses separate components of the developed algorithm, while in the second part evaluates the overall system, in Subsection 6.6. The third part presents the thesis conclusions in Subsection 6.7.

The first systems components to be discussed are the two procedures for generating training and testing data, namely the MOJO and the 4D procedures. Then, the following aspects to analyze include the two classes of Neuro-Fuzzy Inference Systems, and the statistical averaging.

The discussion of each separate systems component is organized to include the following points of interest. First, the role and the main characteristics of each component are underlined. Then, the pressures to develop each special element and how the research goals have been attained are mentioned. In addition, the advantages and the disadvantages or the limitations for each system component are presented. Finally, the section closes with the evaluation of the components performance and the comparison of them with other similar approaches, if they are available.

6.2. MOJO PROCEDURE

The first systems component to be discussed is the MOJO procedure. The scope of this procedure is to generate training datasets that satisfy the desired criteria. As it was modeled in Subsection 3.6, the MOJO procedure includes iterative cycles of data samplings and data rejections, until all the three criteria converge. The motivation for designing the MOJO procedure was cited in Subsection 2.3.

The main goals of the MOJO procedure are reviewed herein:

A. Creation of a training dataset that has the ideal size and it lies within the desired size limits,

B. Increasing the training dataset dispersion,

C. Increasing the comprehensiveness of the training data across the desired data range, and finally

D. Improving the systems prediction performance.

The above goals are directly related to the convergence criteria of the MOJO procedure. This thesis investigates whether the MOJO procedure cures the drawbacks of the Diagnostic System and whether it attains the above goals.

First, the size of the dataset that is derived through the MOJO procedure is within the desired size limits that have been set down in Subsection 4.3. The evidence on this conclusion can be found in Figure 5.1. From the other part, the MOJO-generated dataset is comparatively smaller in size than any randomly sampled dataset that contains the same information intelligence. This became clear in Figure 5.2, because the MOJO dataset contained 160 data versus the 226 accumulated data of the equivalent random dataset. As a result, by using the MOJO-generated dataset, the need for computing resources is reduced, because the training datasets size is reduced. So as only the selected data that include the essential necessary information are loaded into the memory, both the computing time and the response time are decreased.

For this reason, Subsection 5.2.1.2 compares two training datasets, which had the same size. The first dataset was derived through the MOJO procedure, while the second one contained randomly sampled data. By comparing these two datasets in Figure 5.3 to Figure 5.6, it became clear that the MOJO-generated dataset included data that were better dispersed along the desired data range.

By observing the histograms in Figure 5.3 to Figure 5.6, it is observed that both the initial random datasets and the MOJO-generated datasets have normal distribution plots. The main deficiency of the initial datasets was that these datasets did not cover the outer area of the service range, while the MOJO-generated datasets covered the data range in a more comprehensive way. Figure 5.4 provides the better evidence about this fact.

However, in the particular cases of Figure 5.7 and Figure 5.8, by comparing the dataset of the initial 160 accumulated elements with the final set of the 226 accumulated elements, it was found that the prediction error of the checking dataset increased slightly. The explanation is that the checking dataset was more similar to the initial dataset that contained the 160 random elements, rather than to the final dataset. An additional explanation is that the rejection intends to correct the dispersion problem of the training dataset, only. So, by observing the Figure 5.2, Figure 5.7 and Figure 5.8, it should not be a surprise that the rejection ameliorates the datasets dispersion, but it does not improve the performance indices. However, when the algorithm converges, the performance indices are within the desired bounds.

Concerning the data rejection, the following additional comments apply. The three different types of the rejection processes reject data, by intervening on these particular elements that are located in information dense areas. The rejection speeds up the convergence of the algorithm, by filtering out the superfluous data that do not contribute new information. By rejecting these data, the indefinite augmentation of the training datasets is avoided. The MOJO procedure converges fast, as it seems to be particularly suitable for data that are randomly sampled from normal distributions.

Besides meeting the above goals, the MOJO procedure offers some additional advantages. First of all, this procedure performs data preprocessing in an automatic way; so it helps to avoid difficulties that are associated with the manual data preprocessing, which is labor intensive task.

The MOJO procedure prepares and improves datasets for the supervised learning of the Neuro-Fuzzy System. The application of the proposed approach is not necessarily limited to this Damage Diagnostics System, but it might be extended as a universal improvement of the Backpropagation Neural Networks, or of networks that employ supervised learning, in general.

From the other part, the disadvantage of the MOJO procedure is that it might require slightly longer time in order to collect the training data. However, the committed time for generating this dataset is far less than the time that is saved during the operational life of the Diagnostic System. The reduction in training time does not lead in compromise of the training quality for the Adaptive Network, but it increases the systems

reliability. The most important advantage of the MOJO-generated dataset is that it boosts the networks performance and it ameliorates the prediction capability of the diagnostic system.

6.3. 4D PROCEDURE

The 4D procedure, which is discussed in this subsection, aims to generate a Damage Diagnostic Decision (3D) Dataset that complies with two convergence criteria. Because the two criteria are contradicting, this procedure attempts to balance them.

This procedure attempts to balance two contradicting goals. The first goal is to minimize the 3D dataset size, while the second goal is to sample testing data that are relevant with the training data.

The study of the 4D process in Subsection 5.2.2 demonstrated that the 4D procedure converged fast with respect to the two target criteria. The normally distribution of the randomly sampled data boosted the 4D procedure to converge fast, long before reaching the maximum allowed dataset size that requires data rejection.

The convergent 3D dataset had the following characteristics. First, the 3D dataset was bigger than the minimum size. This offered an advantage, because in this way the damage diagnosis decision was based on more than just a few measurements, so the decision reliability increased. The 4D procedure converged when the diversity criteria have been met. In all cases, the convergent 3D set was smaller in size than the training dataset. In this way the detection decision was not postponed for too long, until the 3D set will have attained the size of training dataset, and the bridge damage is identified as early as possible. Therefore, the 4D procedure balanced successfully, between the reliability and the prompt detection response.

In conclusion, the above described MOJO and 4D procedures created the needed datasets for the proper and smooth functioning of the Adaptive Learning Network that is described in the coming subsection.

6.4. NEURO-FUZZY NETWORKS

Two classes of Neuro-Fuzzy Networks have been used. Their common characteristics, advantages and disadvantages are discussed in the following lines.

The first discussion concerns the A-Class ANFIS. The scope of these networks is to predict the excitation force that is required in order to bring the undamaged bridge on a certain given level of kinetic vibration. This predicted excitation force is compared with the actual excitation, in order to derive the damage calculation.

The main benefit of the A-Class ANFIS is that the avoidance of building an analytical bridge model. So, there is gain in the invested time and resources, and in parallel there is a moderate independence from the bridge experts. The Neuro-Fuzzy System does not face a problem when dealing with noisy or sparse data, either. The accuracy of the network is also exceptional. Figure 5.13 shows that the prediction error is very low. An additional advantage is that the ANFIS system provided predictions within a reasonable amount of time. In the case that there is a need for systems modifications or for the additions of new functionalities, or for changes on the type and on the number of inputs, then the ANFIS is capable to treat any other inputs with the minimum adaptations on the Networks topology and on the formulation. This means that the network is plastic and flexible enough to be adapted to new conditions.

The next discussion concerns the twin B-Class Neuro-Fuzzy System. The properties and the advantages of the B-Class ANFIS are similar to the ones discussed above concerning the A-Class ANFIS. So, the reader is referred to the previous paragraphs for a detailed analysis of the general and common characteristics of this systems component. This subsection includes the remarks that apply on the B-Class ANFIS, exclusively.

The scope of this second class ANFIS is to calculate the prediction error that is associated with the A-Class networks. This estimation done by the B-Class ANFIS is used in order to correct the damage rate that is predicted by A-Class ANFIS. In this way, the final subtraction outcome is a new damage rate that takes into account prior information on the predictive uncertainties.

As it can be seen in Figure 5.13, the B-Class ANFIS reduced the damage rate error considerably. However, in certain cases, the final predicted damage rates, which is

corrected by the B-Class Networks, is reduced much more than it should be and it becomes lower than the real value. Therefore, it is recommended to avoid removing this corrective quantity that is the outcome of the B-Class Network. In this way, the predicted damage might be higher that the actual damage rate; however this higher value calculation lies on the safety side.

The use of the B-Class Neuro-Fuzzy system would be beneficial, if the prediction error of A-Class ANFIS was considerable. But, as in our simulation example the A-Class ANFIS exhibited excellent performance; so the use of the B-Class system might be somehow unnecessary.

6.5. STATISTICAL AVERAGING

The statistical averaging aims to provide predictions that exhibit increased confidence and reliability. This process is used in two occasions. In the first case, the purpose is to calculate the mean damage rate of all estimations during the same vehicle event. In the second case, the purpose is to average the damage rates of different vehicle events.

Figure 5.12 concerns the first case, and it shows that the prediction of the damage rates fluctuates considerably, during the vehicle event. It is observed that the predicted damage rate diverges from the real damage 7% as much as a factor of 1.8 percentage units. The prediction is unstable, because the results come from the Neuro-Fuzzy Networks, which are trained with different datasets. As a result, these networks exhibit different degrees of prediction accuracy. However, the average damage rate for the vehicle event is close to the real damage rate.

Figure 5.13 confirms that the predicted damage included a negligible error. For this reason, it is worthless to use the statistical averaging or the moving average technique. Such a statistical method would be used to remove spontaneous results that depart from the average, if the deviation from the mean predicted values was due to bad performance of the learning algorithms. However, if this deviation arises due to suddenly

developed damage in the bridge structure, then using the statistical processes will not be an appropriate choice.

6.6. GENERAL

Up to the present, the Damage Diagnostic System's components have been discussed. This subsection discusses about the integrated Diagnostic System. The scope of this system is to identify and quantify structural damage in civil structures.

Below, the advantages of the Intelligent Damage Diagnostic System are mentioned, by focusing on two key factors that address the system itself; namely the prediction accuracy, and the timely systems response.

The first key factor to evaluate is the systems prediction accuracy. By considering all the damage decision datasets, the average prediction was correct in the 99% of the cases. It is important to mention that the average performance of the Intelligent Damage Diagnostic System, which was calculated through the Monte Carlo Simulation, had a value with indicative and not absolute importance, because it depends on randomly generated data. The high degree of the prediction accuracy would guarantee the correct diagnostic decisions, during the bridge operation.

The second system factor to be discussed is the time duration for the systems response. The proposed diagnostic procedure consumes additional time for collecting the Damage Decision Sets. These sets are completed after the passage of 20-25 vehicle events approximately. From the other part, given the finalized Damage Decision Set, the Neuro-Fuzzy Network completes the required analysis and provides accurate results within a time frame of not more than a few minutes. Therefore, as the Damage Diagnostic System is not only reliable but also it responds in a reasonably fast way, it can be incorporated into practical applications for the Health Monitoring Systems.

Although the Damage Diagnostic System requires training data that are sampled from the undamaged structure, it does not need information and examples sampled from the damaged bridge. The independence of the System from the damaged examples is an

important advantage, because the finalization of the training dataset is taking place, before the damage development on the structure.

However, even if the damage cases are not available to be included in the training dataset, it is not employed an intelligent learning algorithm that is based on unsupervised learning, but on a supervised learning algorithm. Even though ANFIS is trained with undamaged bridge data only, it overcomes this deficiency and it is capable to emulate damage diagnosis. This becomes possible, because ANFIS is trained to recognize the data that belong to the undamaged state, and then the diagnostic system characterizes the bridge as damaged, if its structure signals exhibit deviations from the reference state.

6.7. CONCLUSIONS

The Damage Diagnostic System was tested on a simulated bridge structure that was excited by moving loads. Based on the simulation experiment and the study which was conducted within the scope of this thesis, the following main conclusions are made.

The Damage Diagnostic System includes four main components that are evaluated below. The first component is the A-Class Neuro-Fuzzy Network that emulates the bridge behavior. The second one is the B-Class Network that estimates the prediction error of the first class network. The last two components are the two sampling procedures for obtaining the training and the testing datasets of the above mentioned learning algorithms.

The proposed methodology does not require an analytical modeling of the bridge, as the trained A-Class ANFIS created a non-parametric model of the undamaged structure. When the Neuro-Fuzzy Network is compared with alternate methods, this soft computing paradigm exhibits considerable advantages; the remarkable accuracy, and the flexibility are the main advantages to mention. The Intelligent Learning Algorithm ANFIS have found another successful application in the field of civil engineering.

The B-Class ANFIS was successful in forecasting the prediction error of the A-Class Inference System. However, including the B-Class ANFIS in the overall

Diagnostic System had disputed usefulness, because it might decrease the damage to greater degree than the required one.

Concerning the two procedures for generating datasets, namely the MOJO and the 4D procedures, the following comments apply. By condensing the randomly sampled data, the MOJO procedure produced training datasets that were information dense. From the other part, the 4D procedure collected testing data that were relevant to the testing data space. With the contribution of the advantages that both sampling procedures offered, the involved Neuro-Fuzzy Networks performed in a more reliable way.

In overall, the developed Structural Damage Diagnostic Method was very sensitive in detecting mild linear damage.

REFERENCES

Adeli, H., and Jiang, X. (2006) Dynamic Fuzzy Neural Network for Structural System Identification, ASCE Journal of Structural Engineering, Vol. 132, No. 1, January 2006, pp 102-111.

Atkinson R. C. and Schiffrin R. M. (1968) Human memory: a proposed system and its control processes, in The Psychology of Learning and Motivation, edited by K. T. and J. W. Spence, vol. 2.

Broadbent, D. (1958) Perception and Communication (Pergamon Press, London).

http://www.bartleby.com/66/60/3960.html. The Columbia World of Quotations (1996): Number of Quotation 3960, Columbia University Press (10/01/2007).

Danilatos, D. (2008) Bridge Health Monitoring through Neuro-Fuzzy Architectures, unpublished Master of Science thesis in Civil Engineering, Missouri University of Science and Technology.

Farrar, C., Sohn H., and Worden, K. (2002) Data Normalization: A Key for Structural Health Monitoring, Structural Health Monitoring: The demands and Challenges, Proceedings of the 3rd International Workshop on Structural Health Monitoring, held in Stanford, CA, September 12-14, 2000, edited by F.K. Chang, (CRC Press, Boca Raton, FL), pp 1229-1238.

Hassibi, B., Stork, D. G., and Wolff, G. (1992) Optimal Brain Surgeon and general network pruning, Proceedings of the IEEE International Joint Conference on Neural Networks, vol. 2, pp. 441-444.

Herrmann H.-G. and Streng J. (1997) Problem-Specific Neural network for Detecting Structural Damage, Structural Health Monitoring: Current Status and Perspectives, Proceedings of the 1st International Workshop on Structural Health Monitoring , Stanford University, Stanford, CA, held in Stanford, CA, edited by F.K. Chang, (CRC Press, Boca Raton, FL), pp 267-278.

Hornik, K., Stinchcombe, M., and White, H. (1989) Multilayer feedforward networks are universal approximations, Neural Networks, vol. 2, issue 5, pp. 359-366.

Huntington S. (1996) The clash of civilizations and the remaking of world order (Simon & Schuster, New York).

Jang, J.-S. R. (1993) ANFIS: Adaptive-Network-Based Fuzzy Inference Systems, IEEE Transactions on Systems, Man, and Cybernetics, Vol. 23, No. 3, May/June 1993, pp. 665-685.

Luo, H. and Hanagud, S. (1997) éAn Integral equation for Changes in the Structural Dynamics Characteristics of Damaged Structuresé International Journal of Solids and Structures, v.34, no. 35-36, pp. 4557-4579.

Meyyappan, L., Jose, M., Dagli, C., Silva, P., Pottinger, H. (2003) Fuzzy-Neuro System for Bridge Health Monitoring, IEEE NAFIPS 2003, 22nd North American Fuzzy Information Processing Society, pp 8-13.

MatLab, Release 13, Version 6.5.0.180913a, June 18, 2002, MathWorks, Inc, Natick, Massachusetts.

Masri, S.F., Smyth, A.W., Chassiakos, A.G., Caughey, T.K., and Hunter, N.F. (2000) Application of Neural networks for Detection of Changes in Nonlinear Systems, Journal of Engineering Mechanics, Vol. 126, No. 7, July 2000, pp 666-676.

Ni, Y.Q., Ko, J. M., and Zhou, X. T. (2002) Damage Region Identification of Cable-Supported Bridges using Neural Network-Based Novelty Detectors, Structural Health Monitoring: The demands and Challenges, Proceedings of the 3rd International Workshop on Structural Health Monitoring, held in Stanford, CA, September 12-14, 2000, edited by F.K. Chang, (CRC Press, Boca Raton, FL), pp 449-458.

Shenton III, H.W. and Hu, X. (2001) Damage detection in beams based on redistribution of dead loads, Health monitoring and management of Civil Infrastructure systems: Proceedings of SPIE Series Vol. 4337, Conference held in Newport Beach, USA, March 6-8, 2001, edited by S. B. Chase and A. E. Aktan (SPIE- The International Society of Optical Engineering, Bellingham, WA), pp. 105-112.

http://www.unc.edu/depts/diplomat/AD_Issues/amdipl_16/warburg_II/stearns_clash.html. Stearns M. (2000) Greece and Turkey: The Clash of Civilizations, American Diplomacy, Vol. V, No. 3 (11/07/2007).

Takagi, T. and Sugeno, M. (1985) Fuzzy Identification of Systems and its Applications to Modeling and Control, IEEE Transactions on Systems, Man, and Cybernetics, Vol. 15, pp. 116-132.

The Fuzzy Logic Toolbox user's guide (1999), Version 2, January 1999, MathWorks, Inc, Natick, Massachusetts.

Zu, B. and Wu, Z. (2002) Neural-Networks-Based Structural Health Monitoring Strategy with Dynamic Responses, Structural Health Monitoring: The demands and Challenges, Proceedings of the 3rd International Workshop on Structural Health Monitoring, held in Stanford, CA, September 12-14, 2001, edited by F.K. Chang, (CRC Press, Boca Raton, Florida), pp 1418-1427.

BIBLIOGRAPHY

Aktan, A.E., Catbas, F.N., Grimmelsman, K.A., and Heywood R., Roberts W., Taylor R. and Andersen R., Fitness-for-Purpose Evaluation of Bridges Using Health Monitoring Technology, Transportation Research Record 1696, pp 193-201, 2000.

Dubi A., (2000), Monte Carlo Applications in System Engineering, Wiley & Sons.

Hoon Sohn and Kincho H. Law, "Application of load-dependent Ritz vectors to Bayesian probabilistic damage detection," Probabilistic Engineering Mechanics, Vol. 15, No. 2, pp. 139-153, 2000.

Hoon Sohn, and Charles R. Farrar, "A Statistical Pattern Recognition Paradigm for Vibration-Based Structural Health Monitoring," Smart Engineering System Design, Neural Networks, Fuzzy Logic, Evolutionary Programming, Complex Systems, and Data Mining, St. Louis, MO, USA, November 5-8, 2000 (presenter: Hoon Sohn).

Hoon Sohn, Jerry J. Czarnecki, and Charles R. Farrar, "Structural Health Monitoring using Statistical Process Control," Journal of Structural Engineering, ASCE, Vol. 126, No. 11, pp. 1356-1363, 2000.

Hudnut K.W., Behr J.A.,(1998), "Continuous GPS monitoring of structural Deformation at Pacoima Dam, California", Seismological Research Letters, July/August 1998 issue, vol. 69, No 4, pp. 299-308, Seismological Society of America. [http://pasadena.wr.usgs.gov/office/hudnut/SRL].

Hyzak M., Leach M., Duff K., (1997), " Practical application of GPS to bridge deformation monitoring", Permanent Committee Meeting and Symposium., International Federation of Surveyors (FIG), May 1997.

Lau, C.K., Mak, W.P.N., Wong, K.Y., Chan, W.Y.K. and Man, K.L.D. (2000): éStructural Health Monitoring of Three Cable Supported Bridges in Hong-Kongé, Structural Health Monitoring: Proceedings of the 2nd International Workshop, Edited by Chang, F.-K., Technomic Publishing Co Inc., pp 450-460.

Ljung L. (1997): System Identification Toolbox: For Use with MATLAB, The MathWorks, Inc., Natick, Massachusetts.

Ogaja C., Rizos C., Wang J., Brownjohn J.,(2000), " A dynamic GPS system for on-line structural monitoring".

Rens, K.L., Neimann, Y.M., and Gruber, T. (1999) A Decision Support Tool for Managing Denver's Bridges, [http://carbon.cudenver.edu/~krens/pw_99_klr_www.htm].

Shearer J.L., Kulakowski B.T.; Gardner, J.F. Dynamic Modeling and Control of Engineering Systems.

VITA

Dionysios Danilatos was born in Athens, Greece on October 7th, 1969. He studied in the high schools Luc@e Leonin and 32nd Public Lyceum of Athens. After graduating from high school in 1987, he worked as a broadcaster in local and National radio stations in Greece and joined the Tanks Corp of the Greek Armed Forces. He received his Bachelor of Science in the Civil Works Technology in February 1997, from the Technological Educational Institution of Athens, Greece. During his bachelor studies, he received a European Union grant and attended classes in Environmental Engineering at the Engineering College of Horsens, Denmark. In the summer 1996, he completed a specialized course in Wastewater Process Operations and Maintenance as offered by the City of Philadelphia, PA, USA. In 1996, he interned with Greece's largest geotechnical company Edrasis - Chr. Psallidas, and get involved in the sites of Kifisos River Bridge and Athens Metro. After graduation, he was employed in Alfa Beton S.A. and Air Traffic Control Systems Ltd (owned by the Consortium Hochtief / ABB / Krantz -TKT). He worked in the construction of the New Athens International Airport in civil works including radar towers, auxiliary buildings, mountainous roads, and radar platforms. In year 2000, he received a European Union scholarship and worked as a young researcher in the Civil Engineering Department (DISTART) of the University of Bologna, Italy.

In August 2000, he enrolled in the master's program in the Engineering Management Department at the University of Missouri-Rolla (UMR). He worked as a Graduate Research Assistant at the Smart Engineering Systems Laboratory and at the Center of Infrastructure Engineering Studies. In year 2002, he enrolled in a second master in the Civil Engineering Department, UMR. He received his Master of Science in the Engineering Management at the University of Missouri-Rolla, in December 2007.